Infrared Thermography Based Performance Analysis of Photovoltaic Modules

by

Moyukh Amin
15121039
Galib Hasan
14221019
Isfar Ahmed
14121071
Sukanya Dewan
18221054

A thesis submitted to the Department of Electrical and Electronic Engineering in partial fulfillment of the requirements for the degree of
Bachelor of Science in Electrical and Electronic Engineering

Department of Electrical and Electronic Engineering
BRAC University
April 2019

Declaration

It is hereby declared that

1. The thesis submitted is my/our own original work while completing degree at BRAC University.
2. The thesis does not contain material previously published or written by a third party, except where this is appropriately cited through full and accurate referencing.
3. The thesis does not contain material which has been accepted, or submitted, for any other degree or diploma at a university or other institution.
4. I/We have acknowledged all main sources of help.

Student's Full Name & Signature:

Moyukh Amin 15121039	**Galib Hasan** 14221019
Sukanya Dewan 18221054	**Isfar Ahmed** 14121071

Approval

The thesis/project titled "Infrared Thermography Based Performance Analysis of Photovoltaic Modules" submitted by

1. **Moyukh Amin (**15121039)
2. **Galib Hasan (**14221019)
3. **Isfar Ahmed (**14121071)
4. **Sukanya Dewan (**18221054)

of Spring, 2019 has been accepted as satisfactory in partial fulfillment of the requirement for the degree of Bachelor of Science in Electrical and Electronics Engineering on 25th April.

Examining Committee:

Supervisor:
(Member)

_____

Dr. Md. Mosaddequr Rahman
Professor, Department of Electrical and Electronic Engineering
BRAC University

Program Coordinator:
(Member)

_____

Dr. Saifur Rahman Sabuj
Assistant Professor, Department of Electrical and Electronic Engineering
BRAC University

Departmental Head:
(Chair)

_____

Dr. Shahidul Islam Khan
Professor and Chairperson, Department of Electrical and Electronic Engineering
BRAC University

Abstract

Interest on generating power from photovoltaic (PV) system is increasing day by day. Power generation from such systems is affected by some factors that can be detected in early stage through proper monitoring. Infrared (IR) thermography is a well-known non-destructive technique which can detect localized heating and quantify hotspot area. In this study active thermography has been applied to detect possible anomalies based on the prediction of visual inspection data along with establishing a relation between temperature dependence on possible performance degradation. Then hotspot been detected using python and openCV and area of the hotspot calculated. One of the main findings is that PV modules have some post manufacturing defects which is visually observable. Junction box creates heat that may impact on the module performance. Also difference between hotspot point temperature and the ambient temperature is found increase linearly with respect to module performance degradation. And the hotspot is mostly generated in the gridlines and more area of defect doesn't result in more performance degradation.

Keywords: thermography, hotspot, photovoltaic module, Degradation, contour detection

Dedication

We dedicate this to our dear parents, who have painstakingly supported us through our succession of undergrad degree and on the path of surviving engineering.

Acknowledgement

We would like to thank Md. Mosaddequr Rahman, PhD, Professor, Dept. of Electrical and Electronic Engineering (EEE), BRAC University; for his support, guidance and feedbacks for completion of the thesis. We would also like to thank Mohaimenul Islam, Graduate Teaching Assistant at the BRAC University for helping to simplify and enjoy this whole thesis experience. Thanks in particular to Mr. Atiqul Islam for his thermal camera support.

Table of Contents

List of Tables

List of Figures

List of Acronyms

CCD: Charge-coupled devices

UFPA: Uncooled focal plane array

EL: Electro-luminescence

PID: Potential induced decomposition

IR: Infrared

IRT: Infrared Thermography

I-V: Current vs. Voltage characteristics

SHS: Solar Home System

NDT: Nondestructive Test

PV: Photovoltaic

Chapter 1
Introduction

An increased interest on generating power from renewable sources has led to an increase in solar photovoltaic (PV) system installations worldwide. Power generation of such systems is affected by factors that can be identified early on through efficient monitoring techniques. With these mentoring techniques the safety of a long-term investment can be ensured which in term leads to a better and efficient renewable energy supply. Since investment in Solar PV system is a long term, the prevention and detection of degradation in a PV module as early as possible is very important. This study developed a non-invasive standardized technique for Bangladesh that can detect localized heating and quantify the area of the hotspots, a potential cause of degradation in photovoltaic systems. This is done by the use of infrared thermography, a well-accepted non-destructive evaluation technique that allows contactless, real-time inspection. This study provides the standardized test technique that can help ensure the quality of the PV modules that are being imported in the country before the installation process is done and invoke warranty of the modules when necessary.

1.1 Background

At present, the solar panel, using photovoltaic and silicone solar cell systems to transform radiation to power, becoming more and more popular in the whole world. Moreover, solar panels are the key energy options of future energy on the planet alongside the wind and hydropower, and provide the added benefit of being easier to integrate into the home. Recent gains in popularity and use can be linked to lower installation and operation costs with more practical panels for domestic use in remote areas and larger buildings. However, despite of having guarantee to provide long term service, the PV cell often fails to execute the exact outcome it was supposed to. This kind of incident occurs due to degradation in performance of PV cell. Since this is a long-term investment, therefore it is important to check the quality and find out the cause of degradation in PV cell or modules. There are many ways of ensuring a PV module's quality and efficiency such as field I-V measurement, IR thermography, visual inspection, luminescence imaging and last but not the least, light and electron beam induced current etc.

From visual inspection, we can find the related hotspot in the thermal imaging of the panels. However, using IR thermography to find the cause of degradation is the most

inexpensive, affordable and less laborious method. It is a well-accepted non-destructive evaluation technique that allows contactless, real-time inspection. Using IR camera, thermal images or thermograms of an operating PV module can be easily taken to detect the defects that cause degradation. Also, this is a non-invasive technique that can detect localized heating and quantify the area of the hotspots, a potential cause of degradation in photovoltaic systems. Applying IR thermography method, classified the dominant failure and degradation modes reported over the entire operating life of the c-Si PV modules [1]. However, they didn't follow any standard for the measurements they have done in their studies.

The aim of thesis is to identify the defects of PV modules using IR thermography providing average temperature and relative area to quantify the hotspot. In addition, by using python image processing to do an area calculation and detection of hotspot and relating the performance degradation with the difference of hotspot temperature. Finally, formalizing the process of degradation analysis and building it as a standard measurement to check the quality of PV system.

1.2 Motivation

As solar PV system has become the most popular renewable energy technology, the demand for it has started to increase swiftly with time. This resulted in the exponential growth of installation investment in the worldwide photovoltaic market. In the past decade the global demand for using sun power has increased rapidly, as indicated on the 2017 Renewables Global Status Report, which highlighted that the global capacity for solar photovoltaic grew from 303 gigawatts in 2016 to 402 gigawatts in 2017. In 2017 alone, a total of 98 gigawatts were added, 22 GW more than last year, and this number is growing every year. Global solar PV capacity grew 265 GW in the past five years between 2013 and 2018.Also, Bangladesh government already started the "500 MW solar power mission" to promote renewable energy use to satisfy growing electricity demand [2].On the other hand, SHAKIR-ul haque Khan stated that during the dry season the average sunlight duration is about 7.6 hours a day [3]. Bangladesh therefore has the potential to meet the demand for electricity in all sectors using the solar power system to its benefit.

Recently 5.2 million solar housing systems (about) were installed in Bangladesh at the end of 2017. The custom SHSs have a total capacity of 218 megawatts, with 17 million users in Bangladesh, the second largest customer after India, and 148 million users according to the

"World status report on renewables 2018"[4]. So around 13 percent of the population of Bangladesh have gained power via the solar photovoltaic system. Furthermore, the power age of photovoltaic plants and the resulting restitution time of speculations on photovoltaic plants depend largely on the operating life and electrical execution of photovoltaic modules.

The experience gained from extensive equality control and qualification testing of PV modules in the manufacturing or assembly phases over the past decades has made an essential contribution to minimizing the infant mortality ratio of these components [1]. As a result, although PV modules have characteristic trait such as limited electrical efficiency, they comprise the most robust part of a PV system, typically featuring warranty periods of up to 25 or 30years. Apart from the obvious merit of such long warranty, PV modules technology can become even more attractive for consumers and investors if the energy production cost is further minimized without making fall in durability and reality during operation [5]. However, the long - term implementation and the wide range of PV modules, due to the shortfalls, which occur mainly in the wake of real operating conditions in the (field) area, will be extremely impaired [6, 7].This leads to a certain abnormality in a system characterized mainly by a low power output, temperature abnormality on the modular surface, extreme thermal or mechanical strains and possibly a threatening safety condition for installation [5].

Taking zero-error PV production in consideration, it is turning into quite obvious that the future investors' ultimate objective is to have robust cutting back and if achievable, to have taken away any supply having potential faults that is cause of degrading PV module performance [8].Which is why, at present, in case of handling a large-scale PV plants consisting of lots or thousands of PV modules, on-line detection and effective identification of any possible fault of PV modules underneath operation within the field still remained a technical and financial challenge[7]. By taking measurements of electrical performance, predictable review of PV modules can be a well-established methodology; however, it is restricted fault detection ability. If any abnormality is seen in I –V characteristic or a reduced output of a PV module or PV plant, it will be taken as failure. By taking individual electrical measurements of each module, the physical location of this fault can be identified.

However, PV operators cannot take such an expensive, extended - period approach on the economical PV market. Advanced inspections using optical techniques, on the other hand, have become increasingly common with digital cameras, charged-coupled devices (CCD) and uncooled focal plane array (UFPA), economically efficient detectors. In particular, electro-

luminescence (EL) and IRT imaging include powerful and efficient tools for the qualitative characterization of PV module, not only for the presence of defects in a PV system, but also for accurate detection of their accurate position. In respect to Bangladesh, these tools are feasible and necessary to ensure the quality of PV panels and their usage. With that motivation we aim to use IR thermography as a standard quality inspector of the photovoltaic system. Everyone can use this method without facing any complicated obstacle and know about what percentage of their PV systems are defected and the locations of the defects for which the performance of the PV system have degraded.

1.3 Literature Review

IR thermography has become a formidable tool in inspecting faults in electrical and medical sector. Since the creation of first IR camera in 1956[25] to its first use in 1990. The IR thermography has evolved and proved to be a very useful tool for detecting faults in electrical sector recently as well. There have been studies using IR thermography to find the faults and defects in a PV module in recent years. The use of it pretty dominant in PV field as well.[5],[7-10]. In principle, IRT or thermal imaging refers to nonintrusive detection and measurement of radiation in the form of two or three dimensional pseudo color images of temperature distribution and its imaging by means of appropriate imagers (thermal camera) [9]. For PV applications, IRT field measurement of PV modules is carried out outside, under constant illumination conditions (i.e. clear sky or, in the worst case, maximum 2 okta non - cumulus cloud coverage, preferred) and under MPP conditions, under stationary lighting. The radiance provides heat and power, which in a "healthy" PV module is likely to lead to a homogenous distribution of surface temperatures. Since most failures influence significantly the PV module's heat behavior, the thermal image of the faulty module is inhomogeneous to the distribution of the surface temperature. In other words, information may be provided by IRT for the exact physical and thermal signatures. The defective cell, cell group or module situation showed a fault. Situation of the defective cell, cell group, or module indicated fault occurring. The thermal signing, however, is used to detect power output losses by diagnosing the module in the form of dissipated heat. The fact that thermal Images can be quickly acquired with minimum devices without sensor involvement and without interrupting PV operation in the field makes IRT a further appointment for defective diagnostics of PV modules [1]. However, characterization I - V is still a second but important factor in providing information

about each fault of photovoltaic modules that has been detected and its impact on power output losses.

IR thermography, on the other hand, can detect and diagnose faulty PV modules, both during installation. Infrared radiation is emitted from all objects and proportionate to their temperatures, according to Planck's black body radiation law. Therefore, IR thermography allows the surface temperature and thus the temperature pattern abnormality of the inspected device to be determined. This data is used to assess degradation along with data on the physical component construction and thermodynamic condition of the component. Two approaches to IR thermography are applicable, that is to say, passive and active approaches. The characteristics of interest in passive thermography are naturally higher or lower than the background. A possible problem is indicated by abnormal temperature profiles and the key term is the temperature difference with respect to a reference, often called a ΔT value which is also known as hot spot. Passive thermography is generally quite qualitative as the aim is simply to identify anomalies. In active thermography, however, the inspected specimen must be energized so as to achieve significant differences in temperature as to bear witness to subsurface anomalies [9].

1.4 Scope of the work

The scope of this works mainly deals with degradation both on PV panel surface and also on module components. It relates the I-V properties with the hotspot (i.e. significant temperature difference faults on PV modules) temperature. Which in turn shows a linear relationship between performance degradation and temperature. Furthermore, an algorithm was created to automatically detect the hotspot from a thermal image and calculate the percentage of degradation in terms of area which is later related with performance. This algorithm can be improved in future and be automatically used in surveillance of large PV grids to find the faults.

1.5 Thesis Organization

This thesis book is later on divided into four sections to better observe the result of our studies, Chapter 1 includes the introduction to our thesis as well as the impact of solar photovoltaic in the aspect of the world and Bangladesh. From there this book has dived into the theoretical background of elements related to this study to give a better understanding of the technology and theories that are the base of this work. In Chapter 3 the working experimental setup that was used to perform this standardized study was elaborated. Finally, Chapter 4 contains the findings of this study as a result and analysis.

Chapter 2
Photovoltaic Module and Infrared Thermography

2.1 Introduction

Before performing a proper experimentation to find a suitable testing method standard for PV module in depth study regarding the Photovoltaics and Infrared Thermography is necessary. This chapter focuses on the theoretical knowledge and information that is needed to understand the analysis of a PV module using IR thermography.

2.2 The Photovoltaic Module

A PV module is an electrical energy converting device for radiation. PV module is made up of many parallel wired PV cells to increase the current and to build a higher voltage in series. The module consists of a protection - proof and waterproof material on the front surface with tempered glass and on the r ear side. The edges are screened and an aluminum

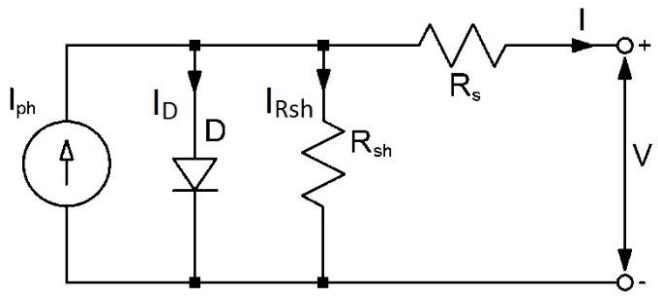

Fig.2.1: An equivalent circuit diagram of a PV cell

frame holds them all together in a mounting unit. All electrical connections are in a rear of the module box. In the figure, the PV cell equivalent circuit is shown. 1 where the I_{ph} current constant source, the light - induced current produced in the cell, is in parallel with the p - n intersection diode. R_s represents series resistance and R_{sh} represents the shunt resistances of the cell. The output current (I) of the PV module can be expressed as equation (1) [14].

$$I = I_{ph} - I_D - I_{R_{sh}} \quad \text{(2.1)}$$

In the above equation, I_s is the reverse saturation current, q is the charge of an electron, V is the output voltage of the PV cell, n is the ideality factor of the p-n junction, k is the Boltzmann's

constant, N_p is the number of cells connected in parallel and N_s is the number of cells connected in series in the module.

On the other hand, A PV module contains large series parallel connections to improve the available voltage. I can be calculated accordingly for a complete PV panel [14] ,

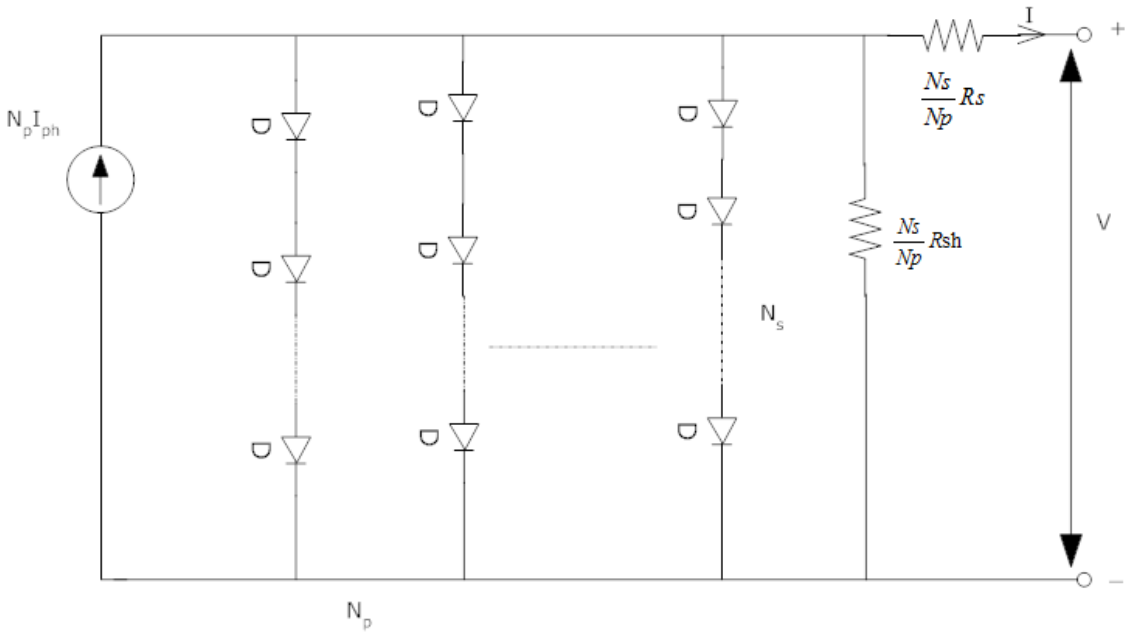

Fig. 2.2: An equivalent circuit diagram of a PV module

$$I = N_p I_{ph} - N_p I_s \left(e^{\frac{q(N_p V + N_s I R_s)}{N_p N_s A K T_c}} - 1 \right) - \frac{\frac{N_p}{N_s} V + I R_s}{R_{sh}} \quad \text{..... (2.2)}$$

Where N_p is the PV cell number that is connected in parallel and Ns the PV cell count connected to each other in series. It should be noticed that several equations are necessary to calculate fully the equivalent PV circuit [24]. Usually each PV cell is considered equal to the rest in the simulation model of a PV panel. N_s and N_p are equal to 1 in PV cell. PV panels usually consist of several PV cell serial connections. If one or more PV cells have a defect, the performance of all PV cells decreases considerably [24].

The intensity emitted from the sun is similar to that of the black body at around 6,000K. Spectral intensity (I_A) is the radiant intensity per unit wavelength where light intensity[2] vary with wavelength. The total intensity (I) is the integration of the spectral intensity (I_A) over the whole spectrum. The integrated intensity above the earth's atmosphere gives the total power flow through a unit area perpendicular to the direction of the sun. This quantity is called Solar

constant or air-mass zero (AMO) radiation which has a value of 1.35kWm^{-2}. In a typical PV cell, light is absorbed through n side causing the occurrence of internal electrical field. Open circuit voltage between the terminals of n side and p side occurs when high frequency photons absorbed within L_h (minority carrier diffusion length) distance and low frequency photos absorbed within L_e distance resulting additional electrons and holes in n side and p side. If external load is added, then the excess electron in n side travels around the external circuit.

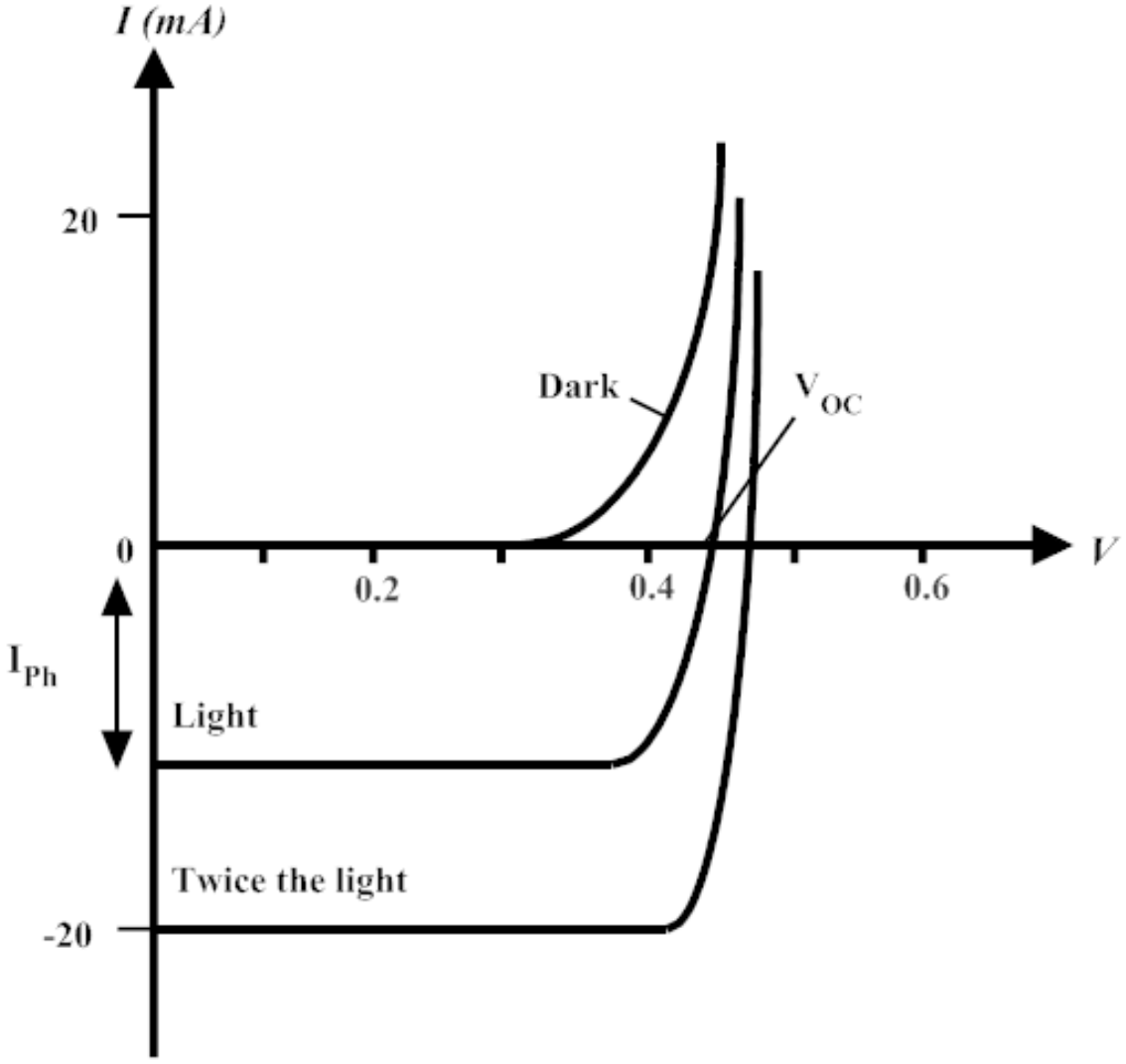

Fig. 2.3: Ideal I-V characteristic of PV cell [15]

Semiconductor	Eg (eV)	V_{OC} (V)	Max J_{SC} (mA cm^{-2})	FF	Efficiency (%)
Si, single crystal	1.1	0.5-0.69	42	0.7-0.8	16-24
Si, poly crystalline	1.1	0.5	38	0.7-0.8	12-19

Table 2.1 Characteristics of Mono and Poly Crystalline Solar Cells, and Reported Efficiencies Under Global Am 1.5 Solar Spectrum (1000 W M^{-2}) At 25°C

When the excess electrons travel around the external circuit, they neutralize the excess holes in the p side. This flow of the photo generated carries creates photocurrent (I_{ph}). Thus, the total current through the PV module [15],

$$I = -I_{ph} + I_o \left[\exp\left(\frac{eV}{nK_bT}\right) - 1\right] \quad \text{(2.2)}$$

Fig.1 shows the ideal Si solar cell I-V characteristic. Here the I_{ph} is the short circuit current and V_{OC} is the open circuit voltage. The I-V curves for positive current requires an external bias voltage. Photovoltaic operation is always in the negative region [15].

From Table 2.1 it can be seen that Solar Si cells, a single crystal that is also known as mono crystalline, have quite high silicone quality and therefore the highest efficiency rates. As these solar panels deliver the highest output power, they also need the least space compared with all other types. Many solar panel companies offer their single, crystal – clear solar panels a 25-year guarantee. However, the most expensive solar panels are monocrystalline. The whole circuit can disrupt when partially the solar panel is covered with shades, dirt, or snow. On the other hand, polycrystalline solar panels are usually slightly less heat – tolerant than single – critical solar panels. However, the efficiency of polycrystalline solar panels however is usually between 13 – 16 percent [16]. Polycrystalline solar panels are not as efficient as monocrystalline solar panels due to their reduced pure silicone quality. Also, their space efficiency is lower. That's why in this thesis 2 monocrystalline and 1 polycrystalline PV modules were used.

2.3 Faults and Hotspots in PV Module

To assess their performance over time and therefore their lifetimes, it is important to identify modes of degradation failure for PV modules. The identification of degradation failure modes on PV modules is important to evaluate their performance along time and so their lifetime. The functioning capability within the suitability standards describes the lifetime of the PV module. Large influx of PV systems worldwide requires a growing demand for laboratories capable of analyzing early degradation and concealed deficiencies in PV modules. The main causing factors for degradation are temperature, humidity, irradiation and mechanical shock. Dismantling causes can be divided widely into three levels: packaging, interconnection and equipment. Typically, product failures are classified into three categories from a lifetime perspective: infant failures, midlife failures, and wear - out failures. Over time, module power

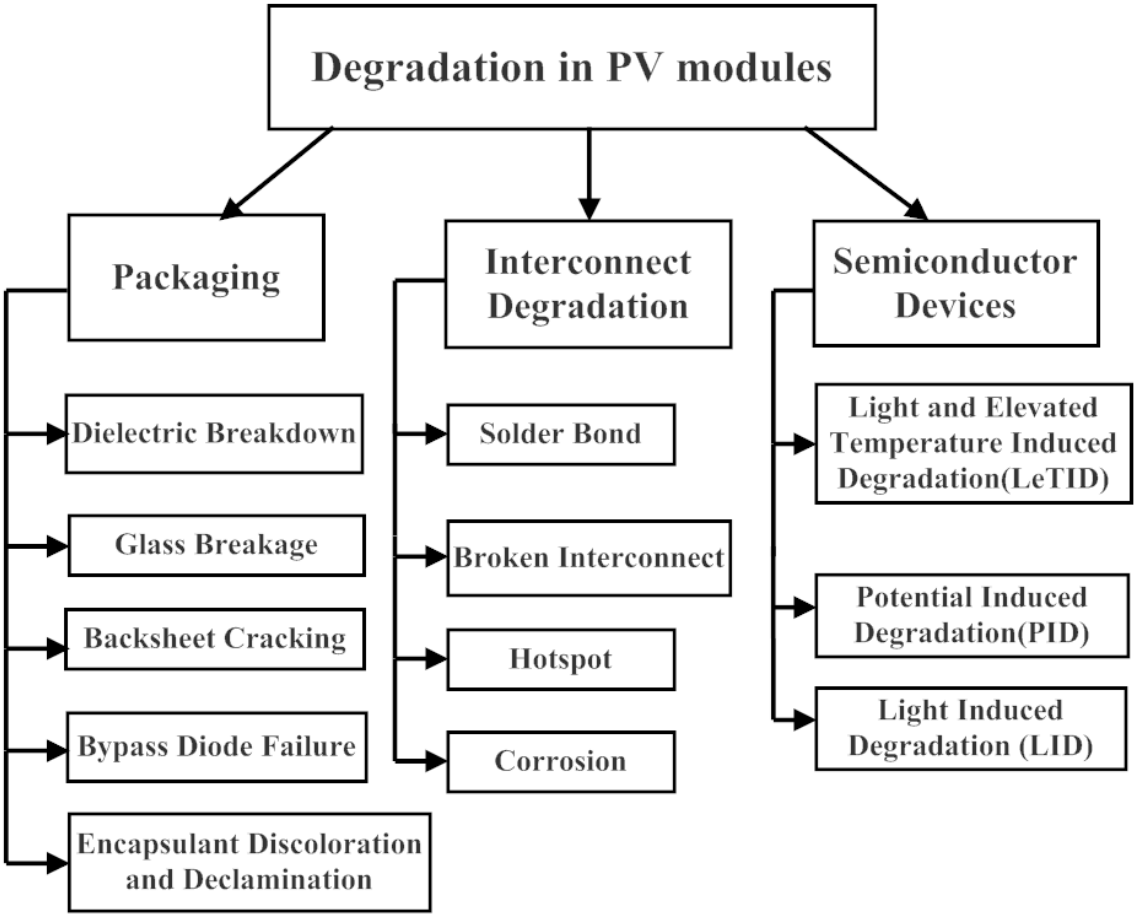

Fig. 2.4: Different possible modes for the degradation of photovoltaic modules from packaging, interconnections and device levels [19]

degradation is built into project expectations and manufacturers warrant. The current 25-year guarantee is typically designed to reduce modules to more than 3% in the first year and 80% of their initial plate power in a linear rate in year 25. [19]. Some suppliers define it as if 80% of the specified power output in standard (STC) test conditions is achieved by the PV panel [19]. Fig. 2.3 shows an elaborated picture of the type of faults that can occur in a PV module.

Packaging

Glass breakage is very common in persistent exposure modules in the field. According to statement of Djordjevic et al [1], this kind of failure occurs due to internal factors like low encapsulation quality, poor or incorrect lamination and external factors, like high temperature. Degradation due to glass breakage can usually be detected by simply visual inspection or even a naked eye before significant losses occur at the power output of the PV module [1]. The result is an undesirable optical reflection and the reduction of sharp solar flux, resulting in a loss of generated current and thus power output from the defective PV module. If the reverse capacity is restricted by voltage or a low shunt resistance reduces the reverse performance, cells can either have a high shunt resistance. Usually the bypass diode reduces the heating incident. If the PV module does not have a bypass diode, the power output will be lost, which will reduce the working PV module's lifetime. Due to damage in packaging, materials become incapable of giving proper service to the whole system and so degradation occurs that cause loss in every knot of the system making its lifetime shorter.

Interconnect Degradation

Hot spot is a term used normally to describe an overheating due to faults in cell. In other words, hotspot is the localized heating phenomena. The most common indicator of solar cell faults, such as cracking, weak soiling, polarization, shading etc. is localized heating. Normally cells display almost uniform current density in reverse bias. In this case the thermal load is distributed over the entire cell and the temperature on the local surface of the cell only increases slightly. Cells that hold a large number of small shunts can usually survive a reverse bias without degradation. Yet, this type of cell will probably exhibit poor current output during cell testing but will not suffer further degradation in the field. By contrast, defective cells with large

shunts can handle current flow via a small silicon area which causes high temperature in a few seconds that can damage the cell. The cell properties eventually suffer damage if the maximum temperature is high enough. Mismatch or broken interconnect occurs in the strings of connected cells cause cells to overheat.

At this moment, reverse biased current occurs in the cells and their junctions have to disperse to adjoining media while the incoming solar energy changed into electrical energy approaching from the other part of the arrangement. Depending on the environment temperature, cells or modules reach a thermal equilibrium. When the balance temperature reaches above the essential value, hot spot occurs. In addition, there can also be hot spots between cells and contact ribbons not or in resistive weld bonds (RSBs). All current must flow through the cell interconnect ribbons and then through distinct solder before finishing flowing in the whole module. Due to field aging, the current fluctuates through a small number of solder bonds rather than all solder bonds failure. Hence, a localized heating at the operating solder bond location occurs due to increased current density. Furthermore, due to corrosion in cells or modules, the power output gets reduced causing loss and degradation.

Semiconductor Devices

Potential Induced Degradation is achieved when the voltage and leakage potential of the module leads to ion mobility within the module between the material of the semiconductor and other module elements such as glass, mount, and frame. Luo et al.19 recently studied PID's causes, shaped the current trajectories of leakages and preventive PID measures in a recent publication. The PID effect can be classified in these categories:

- System level
- Module level
- Cell level

There is a critical distinction between the PV system and the soil at system level. Temperature and humidity environmental parameters are important at the module level. The water interruption into the module increases conductivity and therefore the leakage current. The processing and quality of the basic material are critical at cell level. In large PV systems with silicone crystalline solar cells p - type this effect is stronger. Because the PV module and

its structure are potentially different, electrons may discharge from the grounded wires if the insulation is deficient. This generates leak current and causes a progressive deterioration in performance by this electric current induced by this module. In this study, degradation for packaging, interconnect degradation and junction box have been observed thoroughly. Observation of degradation due to semiconductor devices wasn't done in this study.

On the other hand, three basic mechanisms involve heat transfer, i.e. conduction in solids, convection between a solid surface and a fluid and radiation from solids. All three heat transfer modes are included in the operational PV module. When localized heating in a photovoltaic (PV) module occurs, it is referred to as hotspot [20]. When monitoring with IR camera localized overheating in a PV module is detected as hot-spot, it will have higher temperature compared to rest of the object surface. This might be caused by various kind of cell defects i.e. cracks, cell mismatch, bad soldering etc. During the active approach of IR thermography measurement, step heating thermal stimulation, by means of conductive heat transfer process, is applied to identify defects on the inspected module's surface [1]. It is a useful tool for detecting defects during the manufacturing process. In this method sample module is heated for a specific period of time in a dark environment. The aim is to achieve a temperature difference (3^oC-5^oC) between the sample module and the ambient temperature. It is to be noted that due to convective heat transfer, a slight temperature gradient of 3–5°C is present within PV module. [21]. In principle, a significant difference between these two values, resulting to a ΔT value over 5°C, can be indicative of a hot spot, as a result of a possible defect [14].

2.4 Infrared Thermography and Approach

The process of acquiring and analyzing emitted infrared radiation and generate thermograms to study heat distribution in structures or regions is infrared thermography. Planck's law describes the spectral density of electromagnetic radiation emitted by a black body in thermal equilibrium at a given temperature T, when there is no net flow of matter or energy between the body and its environment [17]. Max Planck later showed how radiated energy emitted at shorter wavelengths increases more rapidly with temperature than energy emitted at longer wavelengths. Planck's radiation is evidently thermal radiation which in terms shows the higher the temperature the higher the infrared radiation. Infrared thermography applies this concept and uses mid-wave (3 to 5μm) and long wave (7 to 14μm) infrared wave sensor to detect the aforementioned thermal radiation to accurately acquire emitted radiation. Then this

radiation is analyzed to generate thermograms that create heat distribution map and superpose it on the original image along with determining the surface temperature all across any inspected

Fig. 2.5: Process of having infrared image of PV modules

body in this study it mapped the heat distribution on the PV modules both on panel side and the junction box view on panel side and the junction box view.

Electro-luminescence (EL) and IRT imaging are powerful and efficient tools for the qualitative characterization of PV module which is standardized by its widespread use and acceptance. The EL imaging is a technique for the on-invasion of carriers that are excited by forward bias in radiography [11]. In short, the resulting light intensity is proportional to the voltage of the normal EL image; therefore, each inactive electric part of a module or cell is displayed as dark regions. [12]. In principle, the presence and place of cell cracks and shunts, possible induced decomposition (PID) and inactive sub - modules (because of bypass shunted diodes or open - circuits), with high precision, can be shown by an inspection of PV modules. [13]. But in many cases of optical degradation and failure, such as delamination or glass (front cover), breakdown, EL-based diagnosis has been very limited or ineffective. This thesis thus used the IRT approach for its inexpensive, portable and fast result. The characteristics of IR thermography is given below:

i) Temperature is captured as a real temperature distribution, and it can be displayed as a visible information.
ii) Temperature can be measured at a distance from any object without contact.
iii) Temperature can be measured in real time.
iv) It has large dynamic temperature range (-50°C – 2000°C)
v) High accuracy (Minimum Resolvable Temperature Difference < 0.1°C)

This thermography approach reflects a recent trend in thermographic NDT development with regard to the use of transient temperature figures [10]. In principle, according to the type of thermal stimulation, there are four active thermographic test procedures:

1. Pulsed thermography
2. Step heating thermography
3. Lock-in thermography
4. Vibro-thermography

Aircraft deficiencies and aerospace components are found in pulsed thermography. Pulsing thermography allows for very rapid inspection of materials for defects and link weaknesses close to the surface. It is a short pulse technique for thermal stimulation. Step thermography is the technique of long-term thermal pulse stimulation. Generating thermal waves through regular heat deposition on the area of the specimen is done by lock-in thermography. Last but not the least; vibro-thermography is the technique where Mechanic vibrations is induced outside the structure leading to friction release of thermal energy.

IR thermography has two approaches i.e. the passive and active approach. In passive thermography, interested areas are naturally at a higher or lower temperature than the background. Abnormal temperature difference indicates a potential defect, and a key parameter is temperature difference with respect to a reference value. This temperature difference is denoted by ΔT. On the other hand, in active thermography, it is necessary to inject current into the specimen inspected in order to obtain significant temperature differences to observe the presence of possible anomalies [18]. In this study active lock in approach of thermography is used to detect the defects.

2.5 Image Processing

A major part of the thermography was detecting the hotspot contour and the area of the contour in relation to the panel area. Contours are the bounding shape that define an area of hotspot on the panel. Contours can be explained simply as a curve joining all the continuous points (along the boundary), having same color or intensity. The contours are a useful tool for shape analysis and object detection and recognition. Basic image segmentation were applied on the thermograms using OpenCV's python implementation to detect these contours.

First, necessary dependencies were imported. The dependencies are cv2 (Open CV Version: 3.3.1), numpy (Version 1.16.2), matplotlib (Version 2.1.1). The image from the IR camera was given in BGR format. The image was pixelated and noise gives false positives in results. So FastN1MeansDenoising was applied. The denoising method is simple. Replacing the color of a pixel with an average of the colors of nearby pixels. The variance law in probability theory ensures that the noise standard deviation is low if most similar pixels are found. The similar pixels to a given pixel have no reason to be close at all. Periodic patterns, or the elongated edges which appear in most images do not show similar pixels in a small window. So a vast portion of the image is scanned to find the most resembling pixel. The resemblance (non-local means) is evaluated by comparing a whole window around each pixel, and not just the color

The parameters of FastN1MeansDenoising that were applied are:

- templateWindowSize: 7, pixels in template patch to compute weights
- searchWindowSize: 21, pixels in window that is used to compute weighted average for given pixel. Should be odd. Affect performance linearly: greater searchWindowsSize means greater denoising time.
- h : 10, filter strength for luminance component, Bigger h removes more noise but also removes image details
- hForColorComponent: 10, same as h but for color components

Thresholding is applied to detect hotspots. The concept is simple, if pixel value is greater than a threshold value, it is assigned one value (in our case white), or else it is assigned another value (in our case black). If pixel value is greater than a threshold value, it is assigned one value (may be white), else it is assigned another value (may be black). The function used is cv2.threshold. First argument is the source image, which should be a gray scale image. Second argument is the threshold value which is used to classify the pixel values. Third argument is the maxVal which represents the value to be given if pixel value is more than (in our case less than) the threshold value. There are many threshing processes but we used binary inverted threshold to separate the pixels.

The function easily explains the graph in Fig 2.4 below. $dst(x,y) = \begin{cases} 0 \; if \; src(x,y) > 0 \\ maxval \; otherwise \end{cases}$

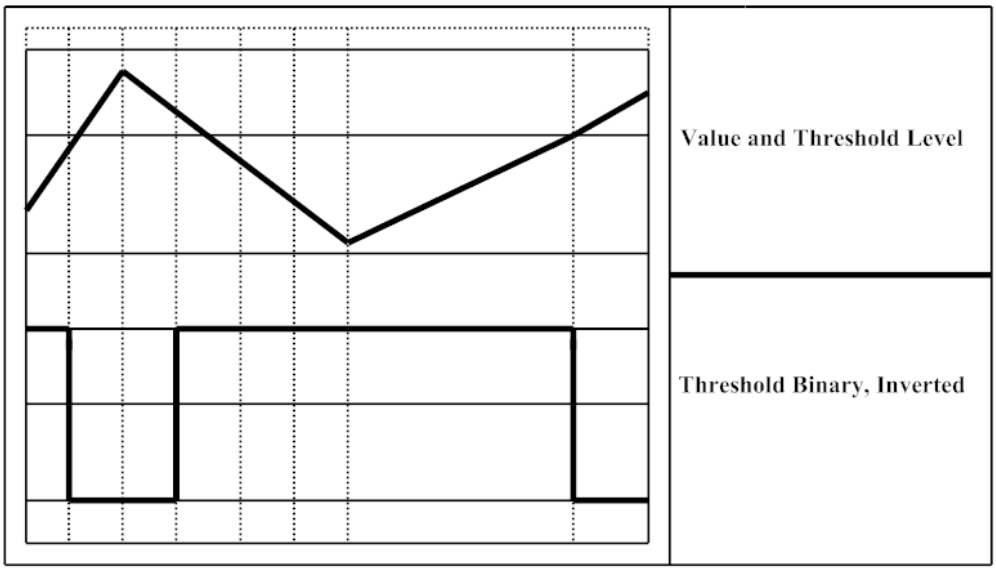

Fig 2.6: Binary inverted thresholding

The function used is cv2.threshold. For that the image was converted to grayscale and the following parameters applied:

- thresholding value 100 is used as only higher red pixels are needed for our study
- maxVal of 255 is used to assign the thresholded value
- Binary inverted thresholding is applied

cv2.findContours is the function used to find the thresholded contours. The output of the function returns an image, detected contours and hierarchy of the contours. The parameters used are:

- Thresholded image as image source
- RETR_EXTERNAL as mode of the contour retrieval algorithm. Retrieves only the extreme outer contours
- CHAIN_APPROX_SIMPLE as the contour approximation algorithm which compresses horizontal, vertical, and diagonal segments and leaves only their end points. For example, an up-right rectangular contour is encoded with 4 points.

Then each contour area was calculated in relation to the image and total area calculated.

2.6 Summary

A basic PV module's structure is explained with its ideal IV characteristics for a better understanding. Also, a discussion of mono and poly crystalline PV module helped further the idea about the characteristics and efficiency of the available module in the market. IR thermography approaches have been elaborated. Then the different faults found in PV module have been discussed with detail in this chapter. Then lastly the logic and the theory behind the image processing area calculation has been explained to show how it worked in this particular case.

Chapter 3
Experimental Setup

3.1 Introduction

A proper experimental setup is crucial to the standard data collection process of a study. Since this study is based of experimental data, the setup of this experiment played a vital role to ensure the collected data's quality. The experimentation was done to capture the panel's hotspot regions, a visual inspection was performed to collect data about the defects on the surface of modules as well. A comparison of the real image of the panel with the IR image of the respective panel has been made possible through these two experimentations and also the module's IR 3D histogram has shown the hotspots in the respective module. The total experimentation process and its setup is sectioned in this part.

3.2 Infrared Camera

All objects emit infrared energy, known as a heat signature. An infrared camera (also known as a thermal imager) detects and measures the infrared energy of objects. The camera converts that infrared data into an electronic image that shows the apparent surface temperature of the object being measured. An infrared camera contains an optical system that focuses infrared energy onto a special detector chip (sensor array) that contains thousands of detector pixels arranged in a grid. Each pixel in the sensor array reacts to the infrared energy focused on it and produces an electronic signal. The camera processor takes the signal from each pixel and applies a mathematical calculation to it to create a color map of the apparent temperature of the object. Each temperature value is assigned a different color. The resulting matrix of colors is sent to memory and to the camera's display as a temperature picture (thermal image) of that object.

Many infrared cameras also include a visible light camera that automatically captures a standard digital image with each pull of the trigger. By blending these images, it is easier to correlate problem areas in the infrared image with the actual equipment or area that is being inspected.

Parameter	Value
IR Resolution	80 x 60
Thermal Sensitivity	≤150mK
Minimum Focus Distance	15cm
Spatial Resolution	7.8mRad
Image Frequency	9Hz
Accuracy	$\pm 2^0$C or 2%

Table 3.1 Specifications of Thermal Imaging Camera

In this study Fluke TiS 10 infrared camera was used to record the IR images of the modules, with the help of IR-Fusion® technology (exclusive to Fluke) which combines a visible light image with an infrared thermal image with pixel-for-pixel alignment. Table 3.1 has the specifications of the Fluke TiS 10 The intensity of the visible light image and the infrared image to more clearly see the problem in the infrared image or locate it within the visible light image. This camera can display the object temperature within the range of -20ºC to +250ºC. Table 3.1 shows the detail specifications of the thermal imaging camera.[23]

3.3. Temperature sensor

The DS1820B Digital thermometer provides 9-bit to 12-bit Celsius temperature measurement and has an alarm function with nonvolatile user programmable upper and lower trigger points [22]. The DS18B20 communicates over a 1 wire bus that by definition requires only one data line (and ground) for communication with a central microprocessor. The DS1820B Digital thermometer provides 9-bit to 12-bit Celsius temperature measurement and has an alarm function with nonvolatile user programmable upper and lower trigger points [22]. It has an operating temperature range of -55°C to +125°C and is accurate to 0.5°C over the range of -10°C to +85°C [22]. In the addition the DS1820B can derive power directly from data line (passive power), elimination the need for an external power supply.

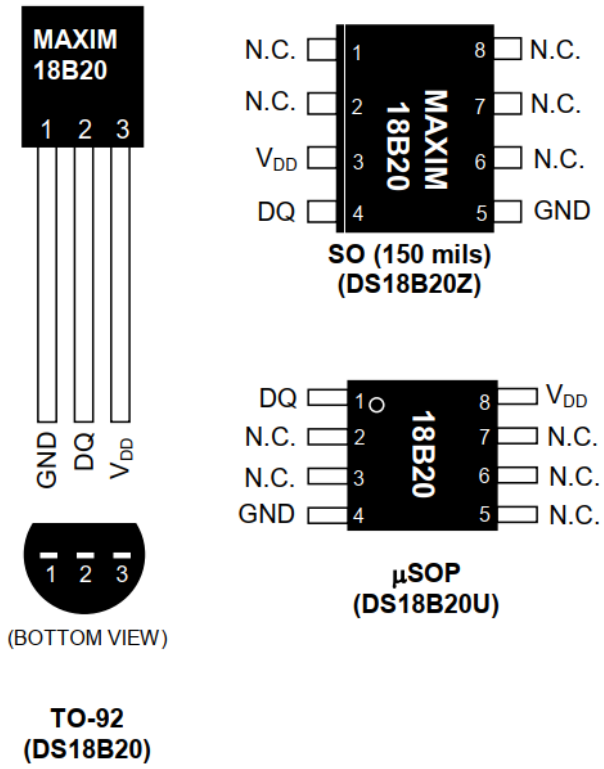

Fig. 3.1: Pin configuration of DS1820B

Each DS1820B has a unique 64-bit serial code, which allows multiple DS1820Bs to function on the same 1wire bus. Fig 3.1 provides a detailed look at the DS1820B pin structure. Thus, it is simple to use one microprocessor to control many DS1820Bs distributed over a large area. Applications that can benefit from this feature include HVAC environmental controls, temperature monitoring system inside buildings, equipment or machinery and process monitoring and control system.

3.4. Indoor testing setup:

In order to perform the *I-V* measurement test under different illumination, a wooden box fitted with ten incandescent light bulbs each of 200 watts as shown in Fig. 3.1(1) was set up. To measure the ambient and the panel surface temperature, digital temperature sensor DS18B20 is used. Figure 3.1(2) shows the connection diagram which is used to record the *I-V*

measurement data of the modules. A 100 ohm rheostat as shown in Fig. 3 is used as the load for the modules. By varying the load resistance, the voltage and current data of testing module are recorded under different temperature and illumination conditions. To get the open circuit voltage, switch S-1 is kept open and to get the short circuit current, both S-1 and S-2 switches are kept closed. For measurements under standard temperature condition, a temperature of 25°C is maintained with the help of room air conditioner. For measurement at higher temperatures, temperature is first allowed to rise to the desired level in the closed box under illumination, and then a fan is used to control the panel surface temperature manually. First, *I-V* measurement data are recorded for two different illumination levels set with four and eight bulbs while maintaining a constant panel temperature. Then *I-V* data were recorded at a fixed illumination while varying the temperature over the range from 25 °C.

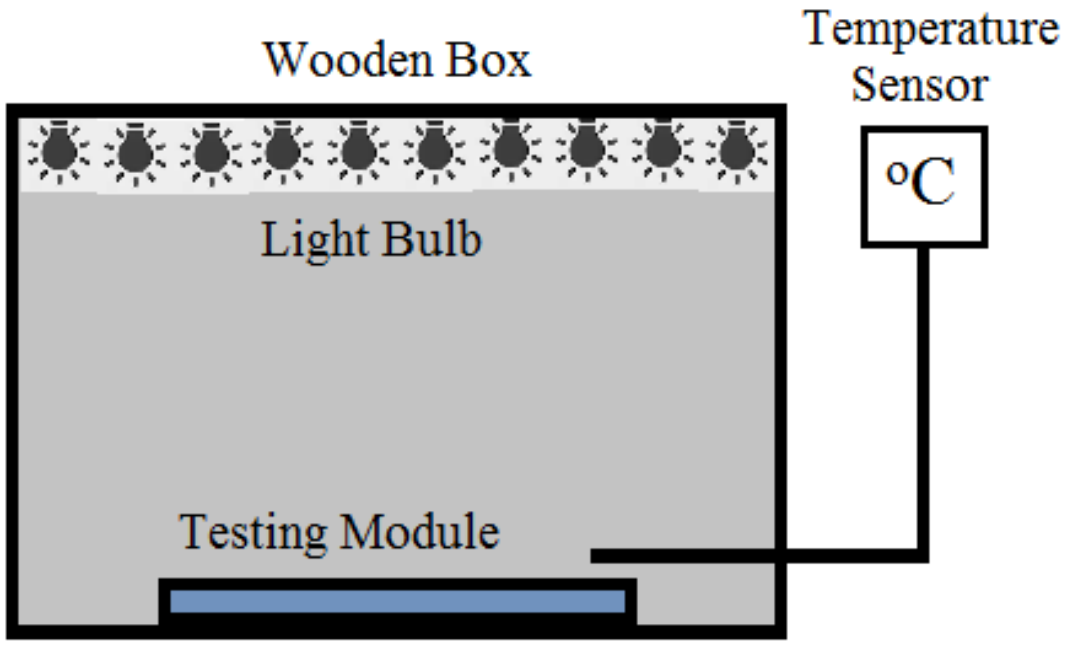

Fig 3.2: Schematic Diagram of Experimental Set Up for The IV Measurement of PV Modules.

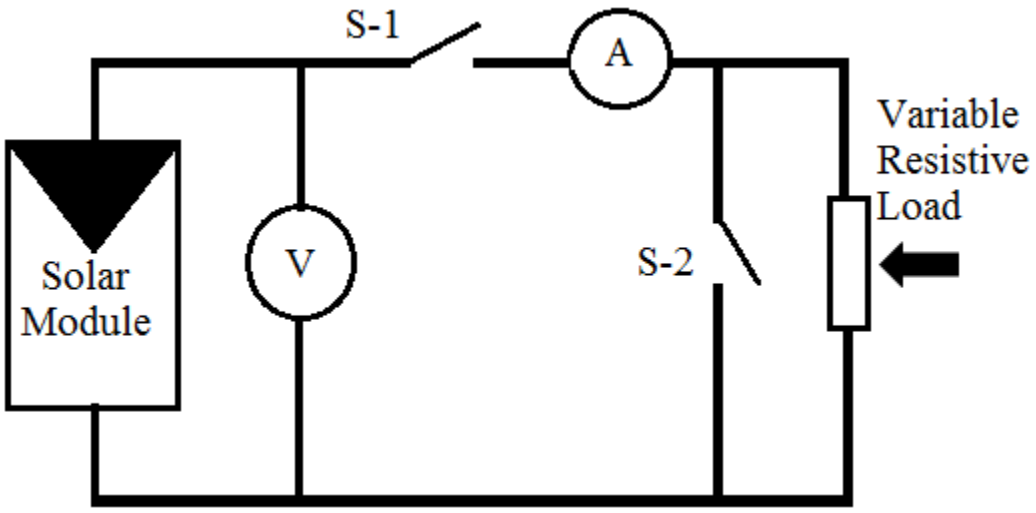

Fig. 3.3: Schematic Circuit of Experimental Set Up Under Illumination

3.5. Supply Condition

At first module was placed into the box. Then it was connected with the DC power supply to provide necessary voltage and current. In this experiment forward voltage was set 23 Volt and the current was supplied 1 Ampere constantly for some time. Images were taken at 1 minute, 5^{th} minute, 10^{th} minute, 15^{th} minute and 20^{th} minute after connecting to DC power supply for the sample modules. Table 3.2 shows the experimental data of the modules. Several images were taken for better quality. After taking images of all the modules, images were analysed in image processing software. Then all the images were matched with the visual inspection data. Furthermore, images were analysed for hotspot area calculation via python.

3.6. Setup

An experimental platform was set up as shown in Fig.3.2 Center to the setup is a wooden box, shown as the shadowed region in the figure, which is used to provide the non-illuminated environment for the sample module. An external DC power supply (30V/3A) was used to provide forward voltage and current to the PV modules. Digital temperature sensor was used to measure the ambient temperature with the help of a microcontroller. Distance between the camera and the PV module was set at one (1) meter. Several images have been taken for each PV sample.

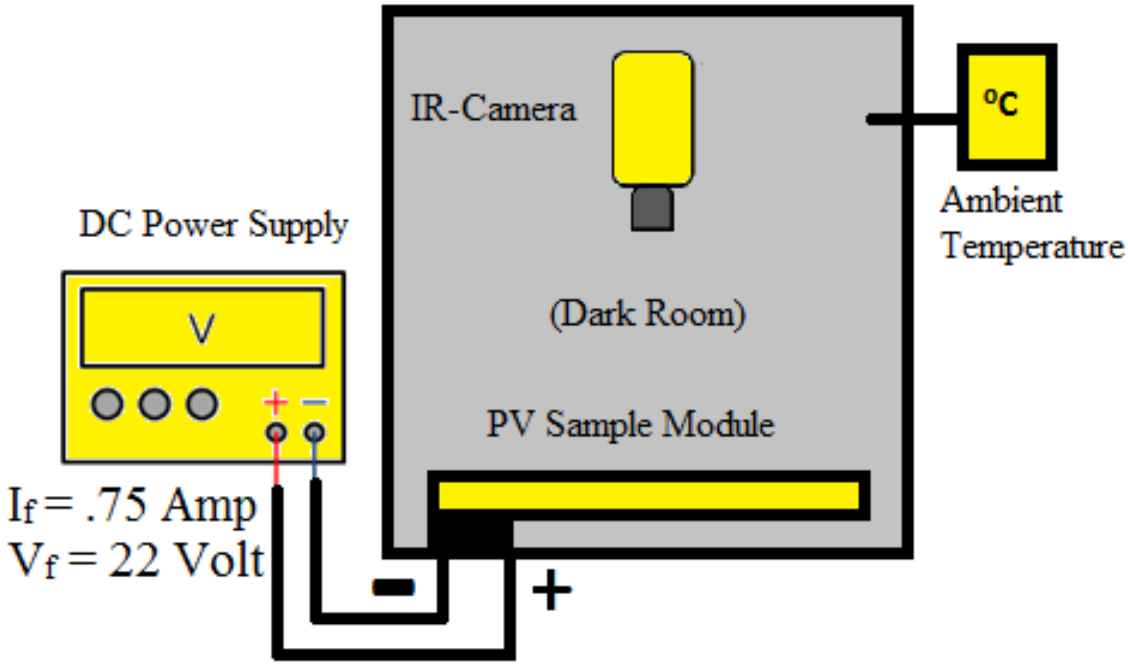

Fig. 3.4: Experimental setup for inspection of PV module

Fig 3.5 shows the photo of experimental setup of PV module before the panel is inserted in the wooden box that creates the dark room condition.

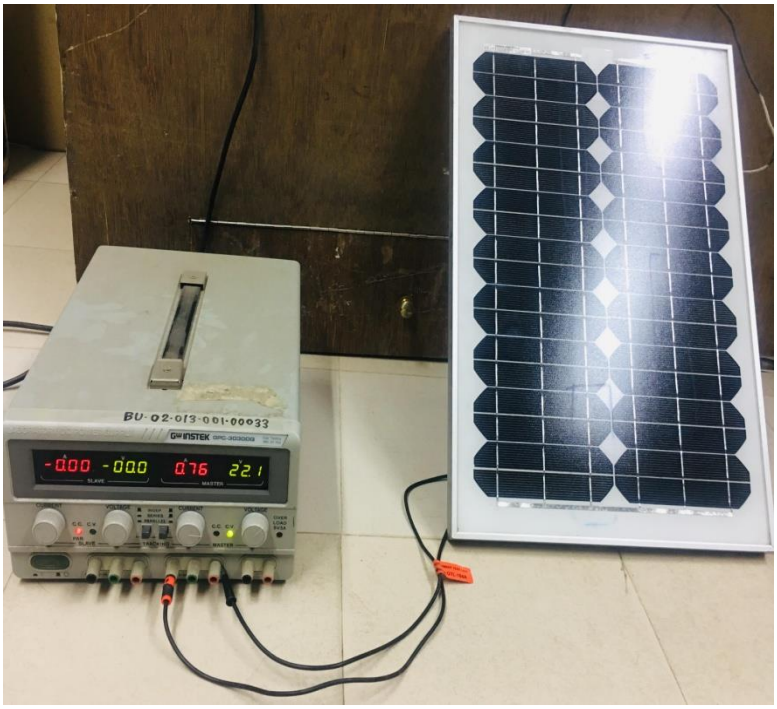

Fig. 3.5: Experimental setup for Module 2

3.7. Summary

The experimental setup is constructed in the dark with the time. In order to keep the room dark the setup would be surrounded with a box so that lights can’t come. So this setup was constructed with a lot of caution and accuracy.

Chapter 4
Result Analysis and Discussion

4.1 Introduction

In this part, the first few sections deal with the conventional performance analysis. The later sections analyze the thermograms of the whole PV module. First, the current, voltage profile that is I-V curve analysis is done. Then visual inspection is done to find visible faults. After which the thermograms of the module junction box shows how solder joints is translated into huge heat loss. Then the infrared images of the panel surface is analyzed and a relation between hotspot and performance degradation is established. In the final part, the area of the hotspot is detected. This was afterwards calculated and visualized on the panel surface.

Parameter	Module 1	Module 2	Module 3	Module 4
P_{mpp}[W]	12.19	10.86	11.38	11.56
V_{mpp}[V]	17.14	17.57	17.45	17.05
I_{mpp}[A]	0.711	0.618	0.652	0.678
V_{oc}[V]	21.40	21.77	21.94	21.83
I_{sc}[A]	0.815	0.685	0.718	0.733

Table 4.1 Experimental Data of Four PV Modules

4.2 Performance measurement of PV modules

Fig. 4.1 shows the *I-V* plots of the sample PV modules, measured with an indoor solar simulator at 25 ^{o}C under the same irradiation level. Table 4.1 summarizes the different PV parameters extracted from the experimental *I-V* characteristic curves of the sample PV modules as shown in Fig. 4.2 From the Table 4.1 it can be seen that the short circuit current and the output power of module 2, 3 and 4 is slightly lower than that of the module 1. This performance degradation is the key indication of possible defects in PV modules.

For the purpose of comparative study, module 1, with the highest maximum power output as per Table 4.1 has been taken as a reference module. It shows that maximum power of module 2 is 10.91% lower than the module 1. So, module 2 is the worst module among the four sample modules. With respect to this sample module, other modules are investigated. The

objective of this investigation was to determine the module degradation and how they affect module efficiency. Also, in order to match the visually inspected hotspot region with this thermal image to find out the possible defects.

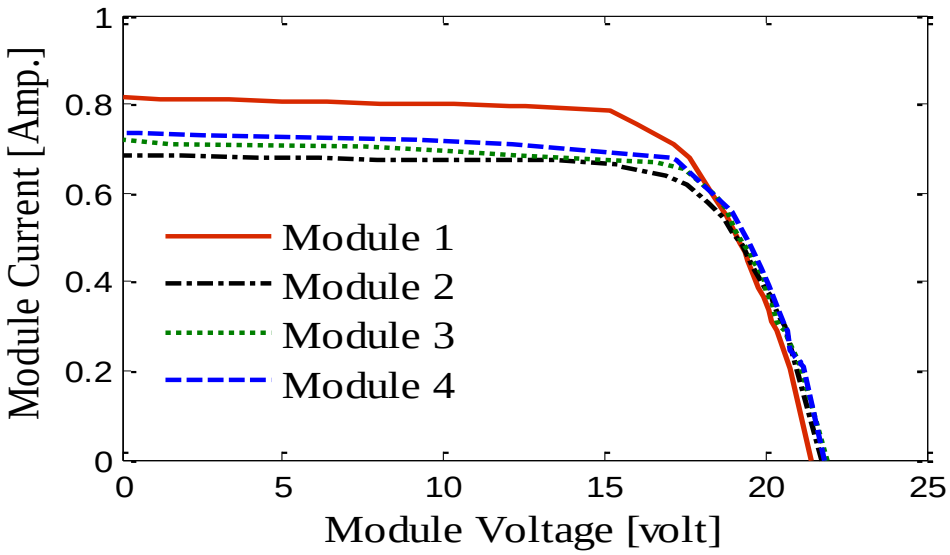

Fig. 4.1: I-V characteristics of 04 sample modules measured at 25°C and under 800 W/m^2 irradiation level.

4.3 Visual Inspection

The PV modules were inspected visually to check for defects. It was observed that most of the PV modules have discoloured cell gridlines in it. The cell cracks were seen in two of the PV modules. Also, some disjointed connection lines between module cells were observed. Resistive solder bonds were observed in all modules. Frames, front glass and back sheets were observed to be in good condition. The results of visual inspection are summarized in table summarized in Table 4.2 possible hotspot region in chalked out as there were some resistive solder bonds in between cell interconnects and some cell cracks in some modules. For further inspection thee possible defected zones are marked.

Error Type	Observation(s)
Cell gridlines	Discolored effects were observed on gridlines of modules 2 and 3. On the other hand corrosion effects were observed on the gridlines of modules 3 and 4
Back sheet	No burn marks, no chalking or other damage was visible
Wires/connectors	No browning was observed
Delamination	No delamination was observed
Cell Gaps	No encapsulation and brown discoloration were observed.
Frames	There was no discoloration or any corrosion was seen on metal joints
Metallization	Bus-bar and cell interconnects showed no burns, discoloration or corrosion
Junction box	No Browning was observed
Interconnect Ribbons	Interconnect ribbons were all okay
Front Glass	No damage, no animal dropping or dust particles were observed
Bypass diode	Bypass diode was unavailable on module 2
Cell crack	Cell cracks were observed on module 1 and 2
Resistive solder bonds	The cell interconnects of all modules were observed possible resistive solder joints

Table 4.2 Visual Inspections of PV Modules

4.4 IR thermography: Module Junction Box

Localized heating may take place in a faulty junction box. To find this, active approach was used to determine which junction is resistive. Fig. 4.2 shows thermal images of two sample module's junction box which were tested under dark condition in forward bias. The ambient temperature was kept 25^{o}C. Here in this approach 23 volt and 1 ampere current was applied to the modules for 60 seconds. From Fig. 4.4 it is observed that junction box of module 2 and module 3 create hotspot. Temperature of the encircled hotspot regions of module 2 and 3 are 29.4^{o}C and 30.1^{o}C respectively. This temperature is much higher than the ambient temperature. The probable reason behind the rise of temperature is heat loss due to resistive joint. This was perhaps one of the main reasons of performance degradation of solar PV modules.

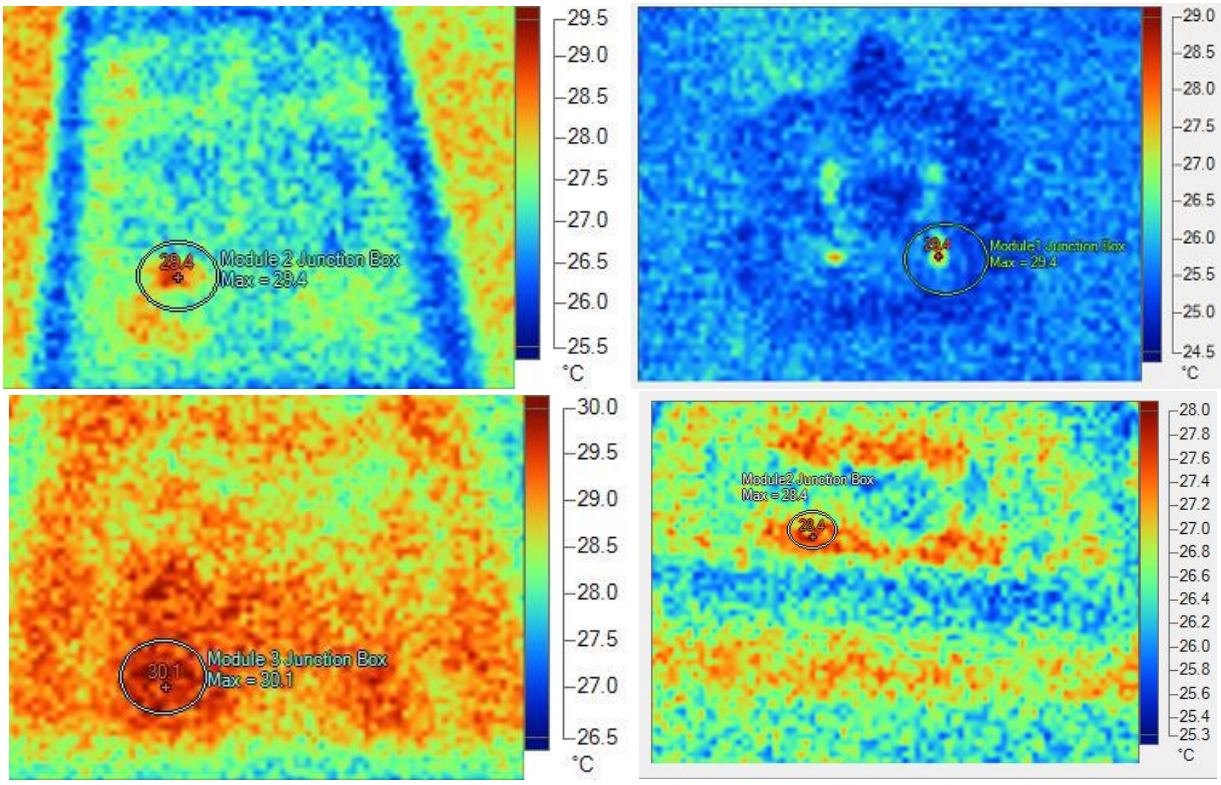

Fig. 4.2: IR thermal image of module 2 (top) and module 3 (bottom) junction box indicates hotspots

4.5 IR thermography: Module Surface

Figure 4.3 shows (a) the IR thermal image of module 1 and (b) the 3D view of temperature distribution on the module surface. It shows that cell interconnector of module 1 shows hotspot. Beside the interconnectors, temperature distribution is moderate. Solar cells within the interconnecting regions shows high temperature. Circle indicates the hottest region which is the probable hotspot area. The ambient temperature during the test was 26.1^{o}C and the highest Temperature in hotspot region was 29.3^{o}C. Temperature difference is 3.2^{o}C for module 1 for the marked region.

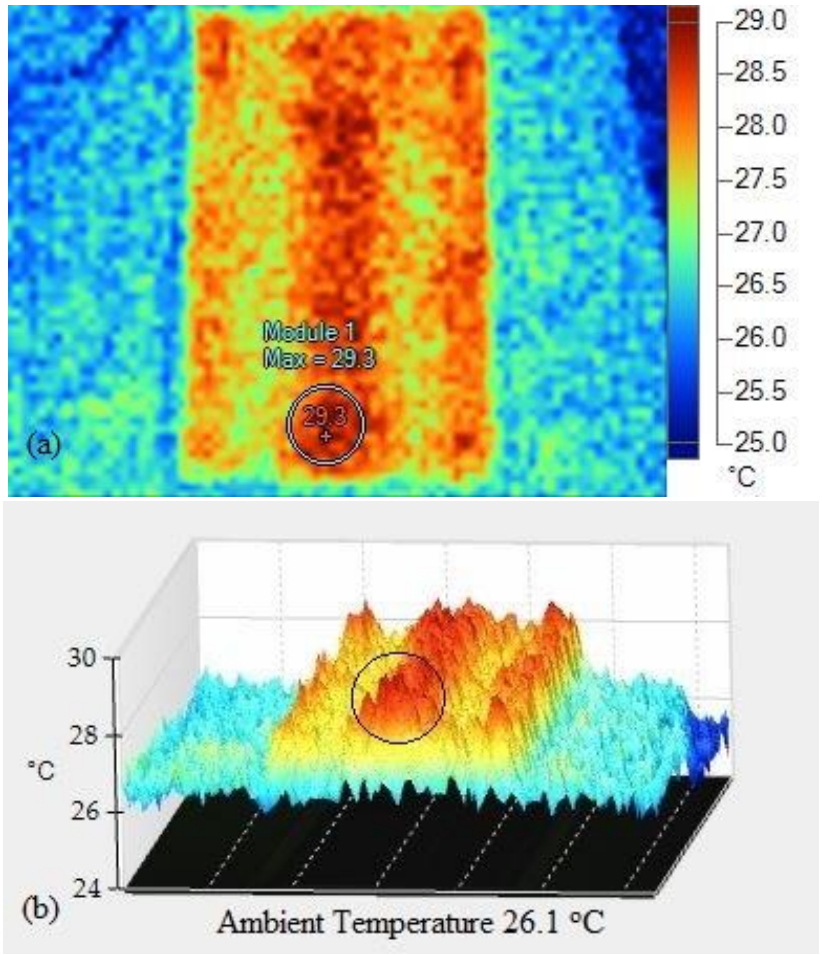

Fig. 4.3: (a) Thermal image of module 1 (b) 3D diagram of surface temperature distribution.

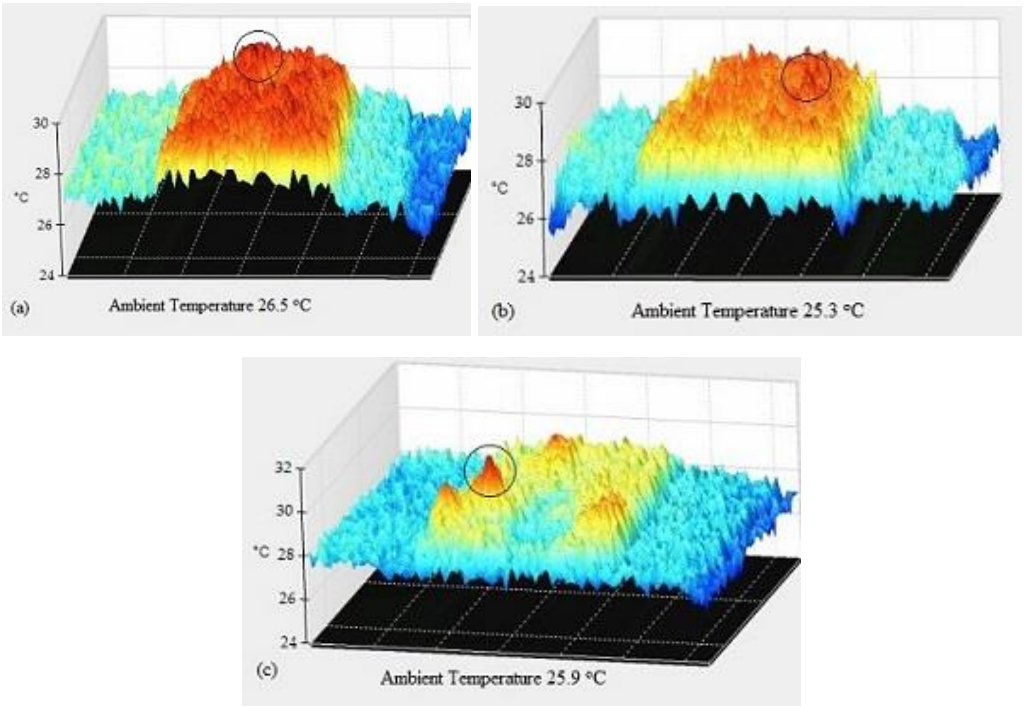

Fig. 4.4: 3D diagram of surface temperature distribution of (a) module 4 (b) module 3, (c) module 2

Figure 4.4 shows the 3D temperature distribution image of (a) module 4, (b) module 3 and (c) module 2. The module 4 demonstrates a slightly lower performance (-5.16%) than the reference module 1. 3D image shows that cells and interconnectors create hotspot. From visual inspection data some possible area of hotspot region is found which are similar to this IR image. The ambient temperature was 26.5^{o}C and the hotspot region temperature difference is 3.7^{o}C marked by the circle. Module 3 shows 6.64% less power output than the reference module. 3D image also shows hotspot region in the cell interconnectors as like module 4. Ambient temperature was 25.3^{o}C and temperature difference is 4.5^{o}C on the marked region. However, it can be seen from the Fig. 4.4(b), IR radiation is more intense on the right side for the module 4, Indicating more heavily resistive solder joints are likely to be present between the cell interconnectors. The output of module 2 is lower than the reference module by 10.91%. The Fig. 4.4(c) shows several hotspots in this module. Probable resistive connectors and visually observed discolored cell gridlines are the main cause of the hotspots. Also, this module shows highest ΔT value over 5^{o}C in the marked hotspot area which represents serious defects occurred in this module 2.

It is observed that as the performance of the PV modules gets worse, the temperature of the hotspot region increases. There seems to be a correlation between the difference in

temperature in the hotspot region and the performance of PV modules. Figure 4.5 shows that the difference in temperature between ambient and hotspot temperature is perhaps linearly increased with performance degradation of PV modules. To understand the relation linear curve is fitted. It shows that when the percentage of performance degraded, temperature difference is increased in marked hotspot region of PV modules. The more the degradation, the more the temperature differences. Also, the temperature maintains a linear rise up. The panels were provided with 1A and 23 volts for a different time frame.

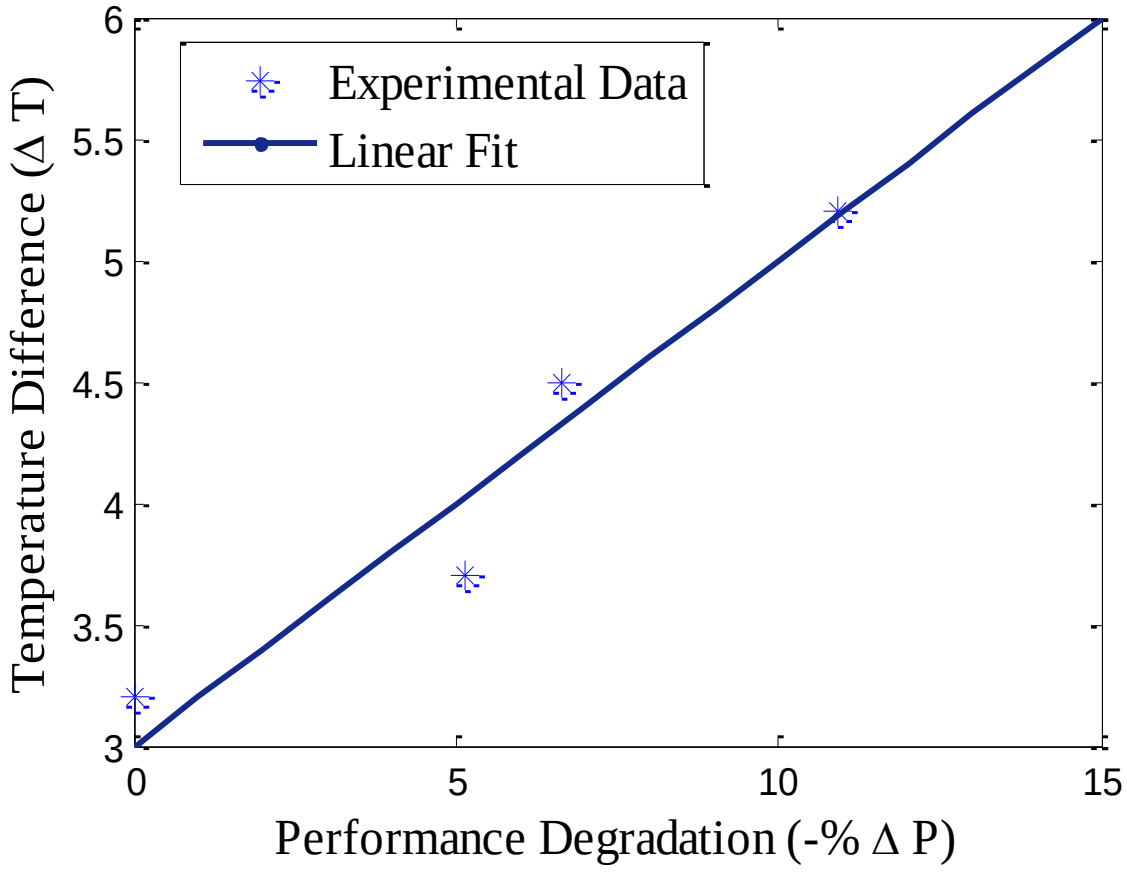

Fig. 4.5: Temperature difference between hotspot and the ambient temperature with respect to performance degradation

The images in Fig. 4.5 are of the same PV module that has been supplied with same voltage for different time, the first image that was taken after a minute has passed and the second image had been taken after 20 minutes. Module 2 after one-minute had the maximum temperature of 29.5^{o}C in the marked region and after 20 minutes it increased to 39.6^{o}C. Temperature differences (ΔT) found with respect to the ambient temperature after 1 minute 20 minutes are respectively 6.5^{o}C and 17.6^{o}C. Similar experiment was done on the other modules, and from there it was observed that the Temperature increase (ΔT) somewhat linearly with

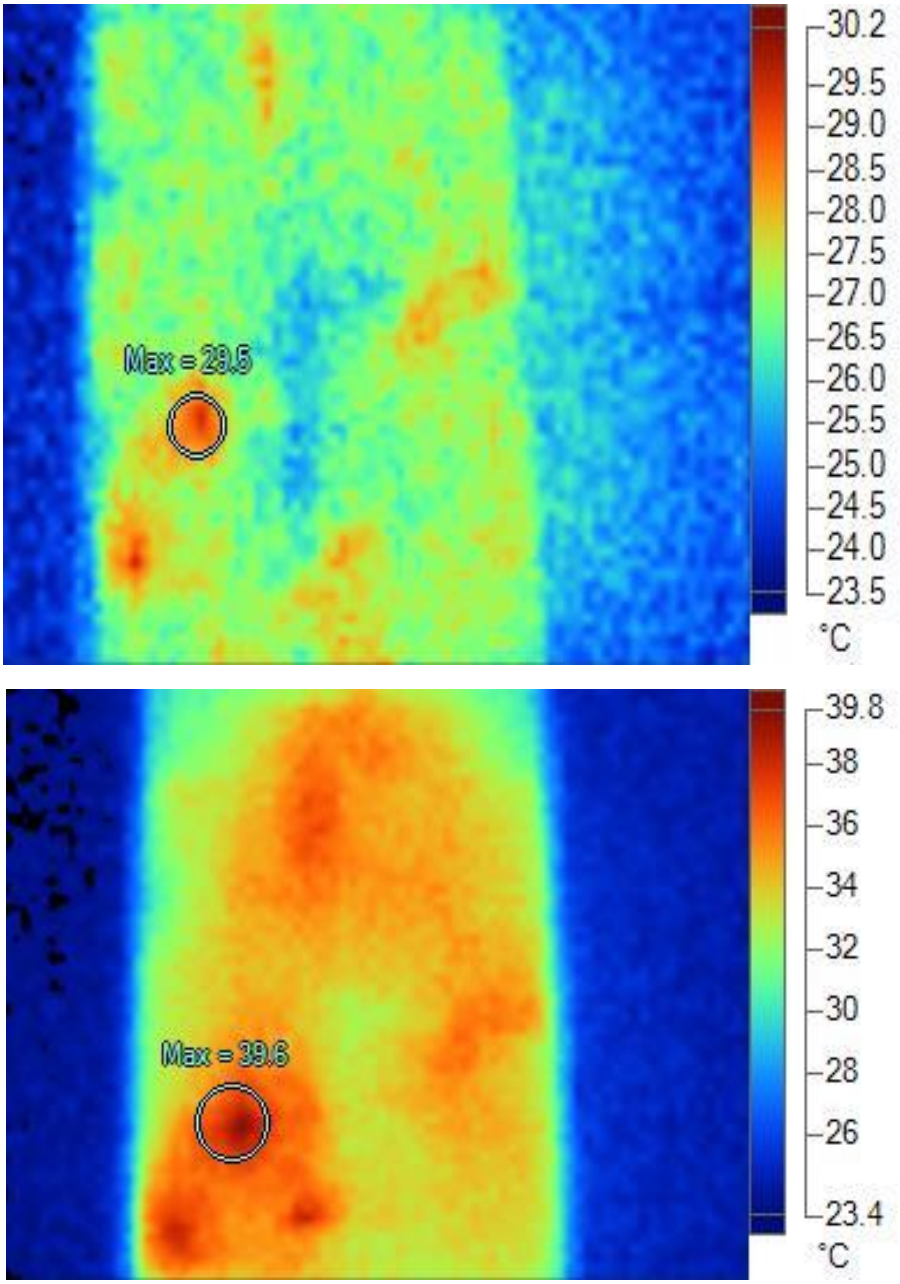

Fig. 4.6: Thermal images of module 2 taken after (a) 1 minute (b) after 20 minutes

respect to time on the same marked hotspot zone. The effect of ΔT was also observed with respect to the percentage of performance degradation, the modules had a higher percentage of degradation as the ΔT increased. ΔT linearly increased as the amount of performance degradation of PV modules increased. Average ΔT increase rate for data taken at a specific time: 0.45°C/Percentage of Performance Degradation.

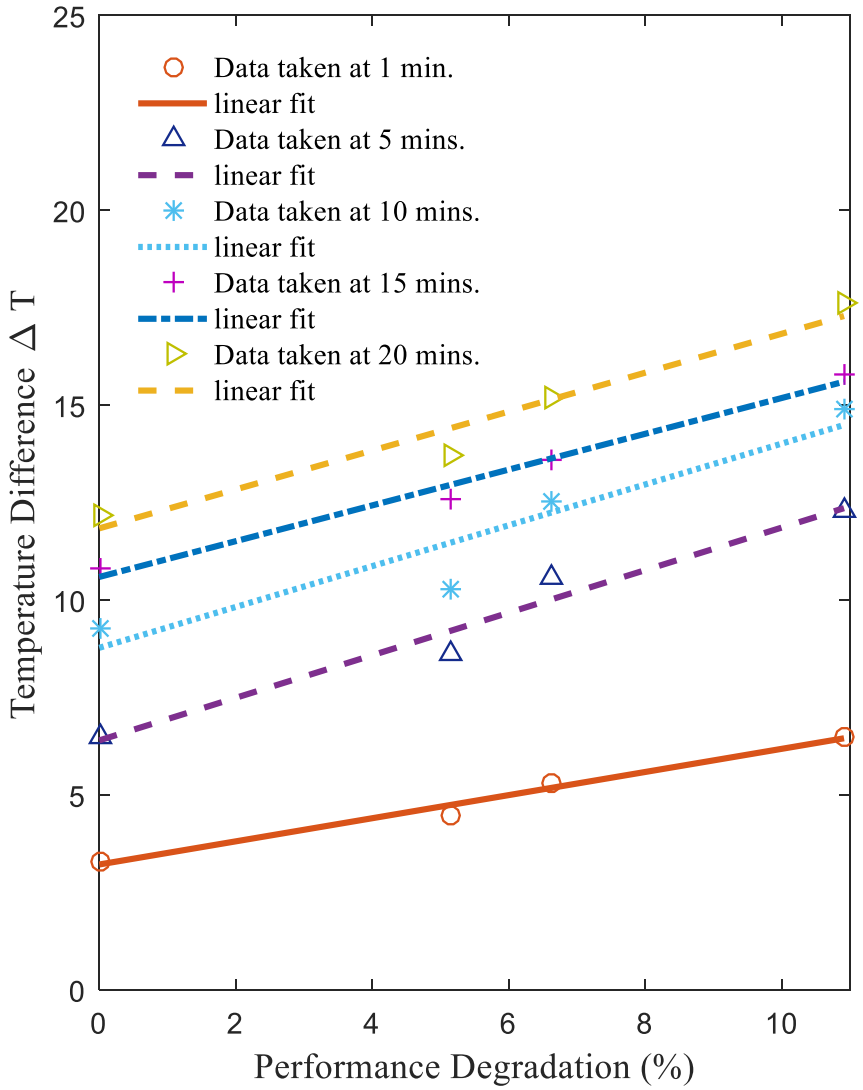

Fig. 4.7: Increase in ΔT with respect to with performance degradation (%) in a linear manner

The ΔT increase rate was 0.53 ^{o}C / Minute in this study. Result of this can be seen in the Fig 4.8, all the modules have a linear increase in temperature over time.

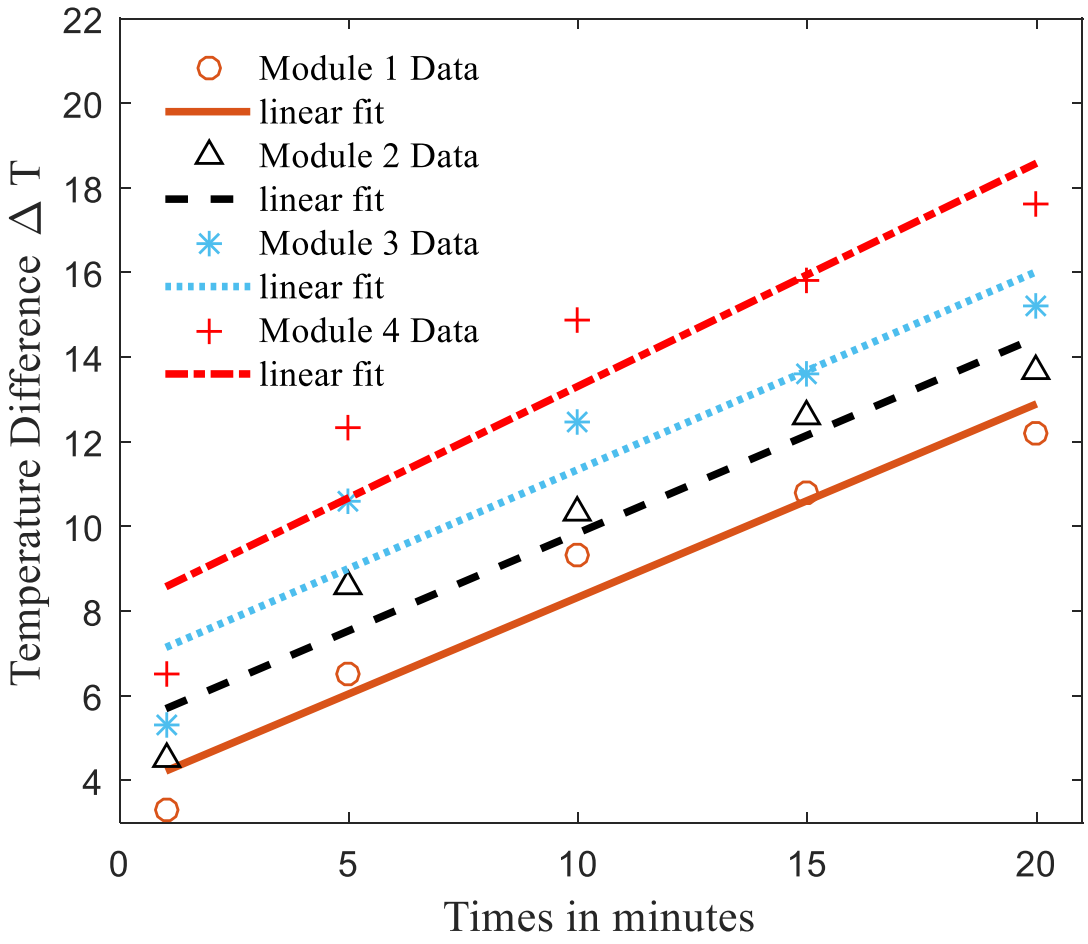

Fig. 4.8: Increase in ΔT with respect to time in all modules in a linear manner

4.6 Area detection and Hotspot Visualization

In the last part of the thesis, an algorithm was implemented to detect the hotspot on the panel from its digital infrared image. Along with detection, the percentage degradation was found and the largest hotspot was visualized over the PV module.

4.6.1PV Module (Poly-silicon 1)

The infrared image of this panel reveals numerous hotspots along the middle but it is perceivable that not all of them are hotspots with the highest temperature. Thresholding was applied and contours detected which shows prominent hotspots not only in the middle but also on the left face of the panel.

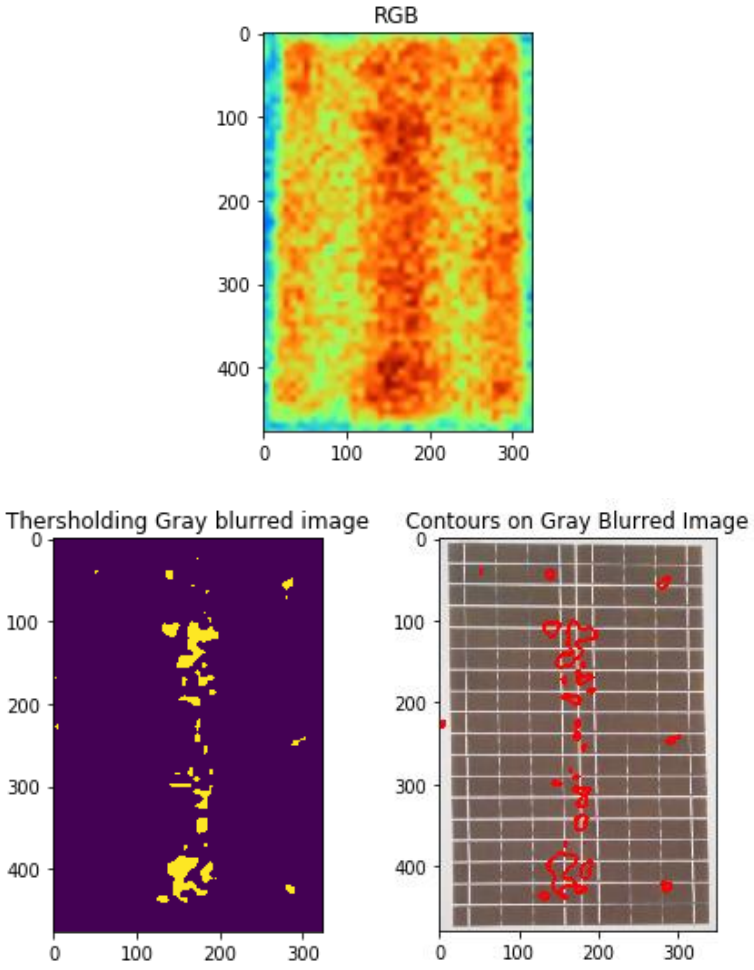

Fig.4.9: RGB, Thresholding Gray Blurred Contours and Gray blurred images of Poly-Silicon 1 PV module

Plotting the contours on the real PV panel image points to a possible defect in the center gridline and visual inspection showed misalignment in the gridlines. Furthermore, the area calculation showed that the largest hotspot was 0.7244582043343654 % and all hotspot totaling to a 2.5465211015153986 % defect on the panel contributing to a power loss of the module.

4.6.2 PV Module (Poly-silicon 3)

The P3 PV module shows 4 probable hotspots. But only one of them has a temperature difference. So, applying thresholding shows exactly that. Contours were detected and shows a defect of 0.4905053105889926 %.

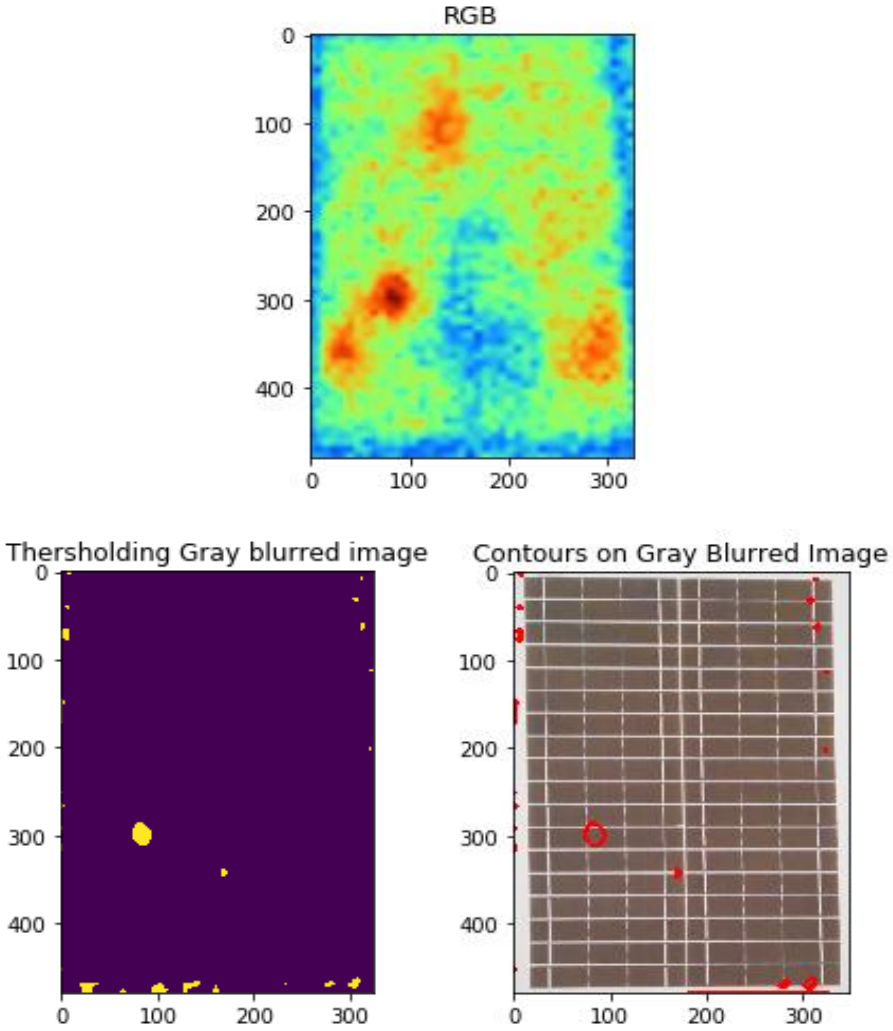

Fig.4.11: RGB,Thresholding Gray Blurred and Contours on Gray blurred images of Poly-Silicon 3 PV module

When visualized it shows the problem lies in a single cell of the module which contributes to the power loss of this PV module.

4.6.3 PV Module (Mono-silicon 1)

The infrared image of this PV Panel shows an even distribution of hotspots only some of them reveals a hotspot with the highest temperature. Applying thresholding reveals major hotspots on the right face of the panel. But a lot of noise was generated due to camera encoding conflicting with blue and red values which can be removed.

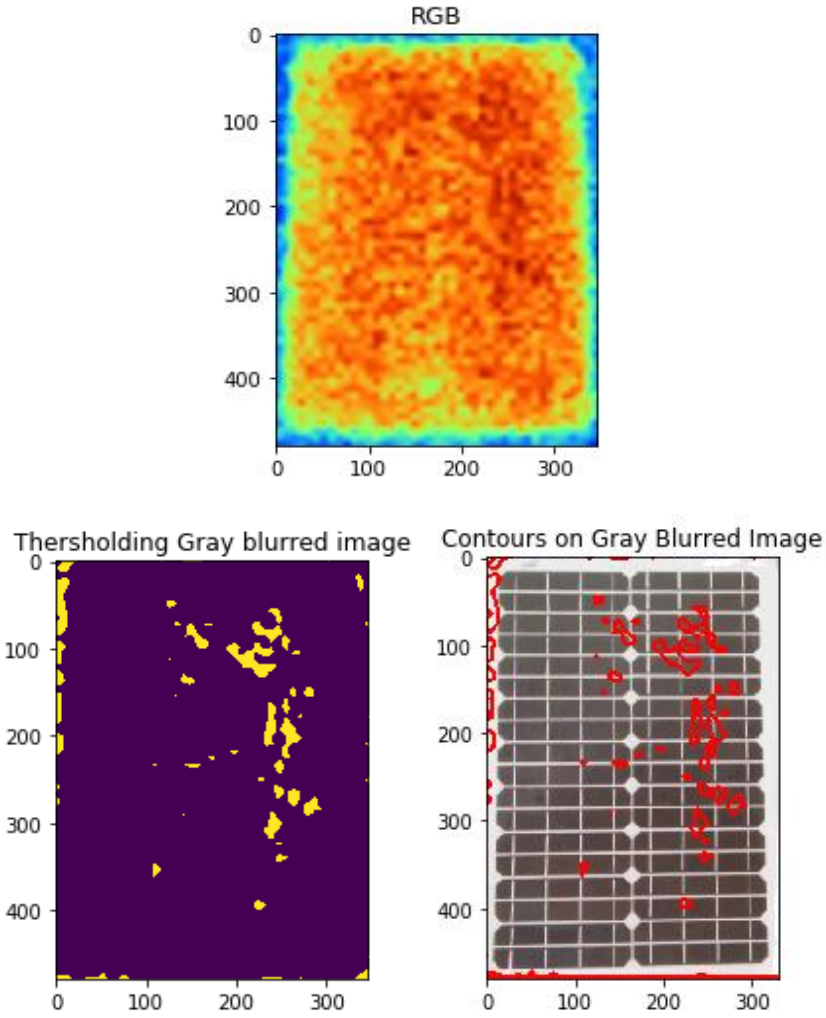

Fig.4.11: RGB, Thresholding Gray Blurred and Contours on Gray blurred images of Mono-Silicon 1 PV module

Detecting contours shows the largest hotspot of 0.5221029652537748 % while totaling to a defect area of 3.5992359468801163 %

4.6.4 PV Module (Mono-silicon 2)

The infrared image shows an even distribution of temperature along the PV Module and sparse hotspots all over. Then applying thresholding shows huge hotspots with maximum temperature.

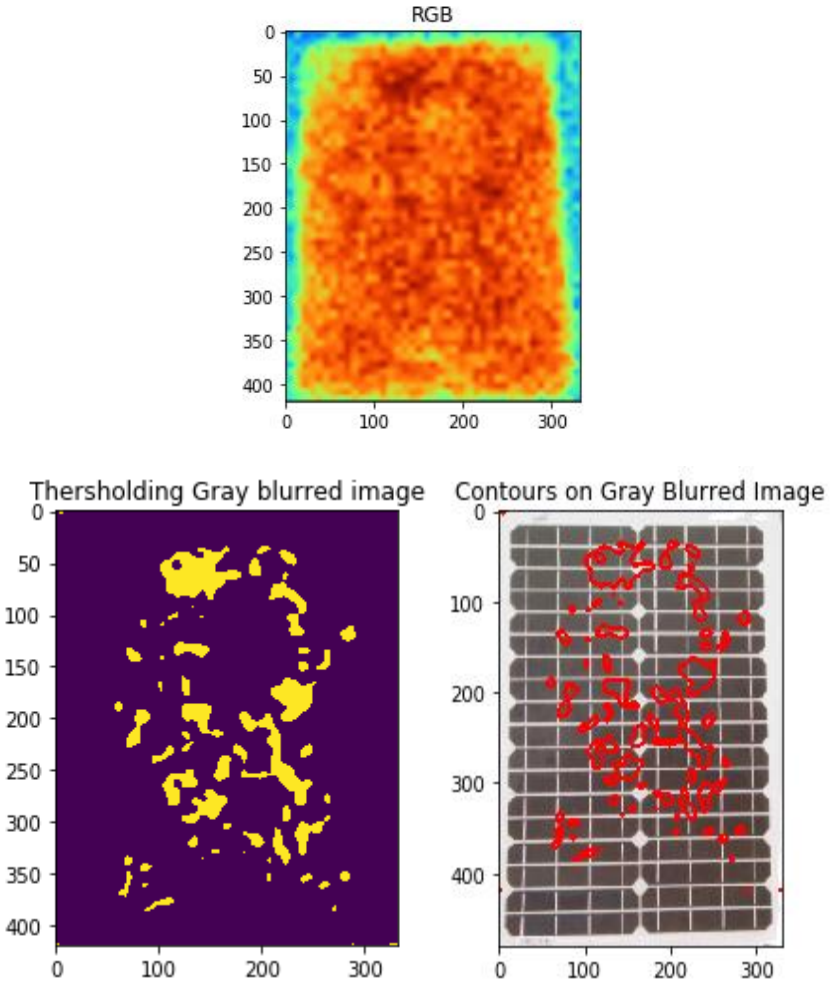

Fig.4.12: RGB, Thresholding Gray Blurred and Contours on Gray blurred images of Mono-Silicon 2 PV module

And on contour detection it was found that a total of 8% defect with the largest hotspot having an area of 1.6% of the total panel. Visualizing on the panels shows one

common feature i.e. most of the hotspots are centered along cell gridlines but unless gridlines are resistive hotspots shouldn't be there.

4.6.5 PV Module (Mono-silicon 3)

The IR image shows a hotspot on the top right. Visual Inspection showed a cell breakage at the same location. Thresholding generates noise but identifies the hotspot accurately.

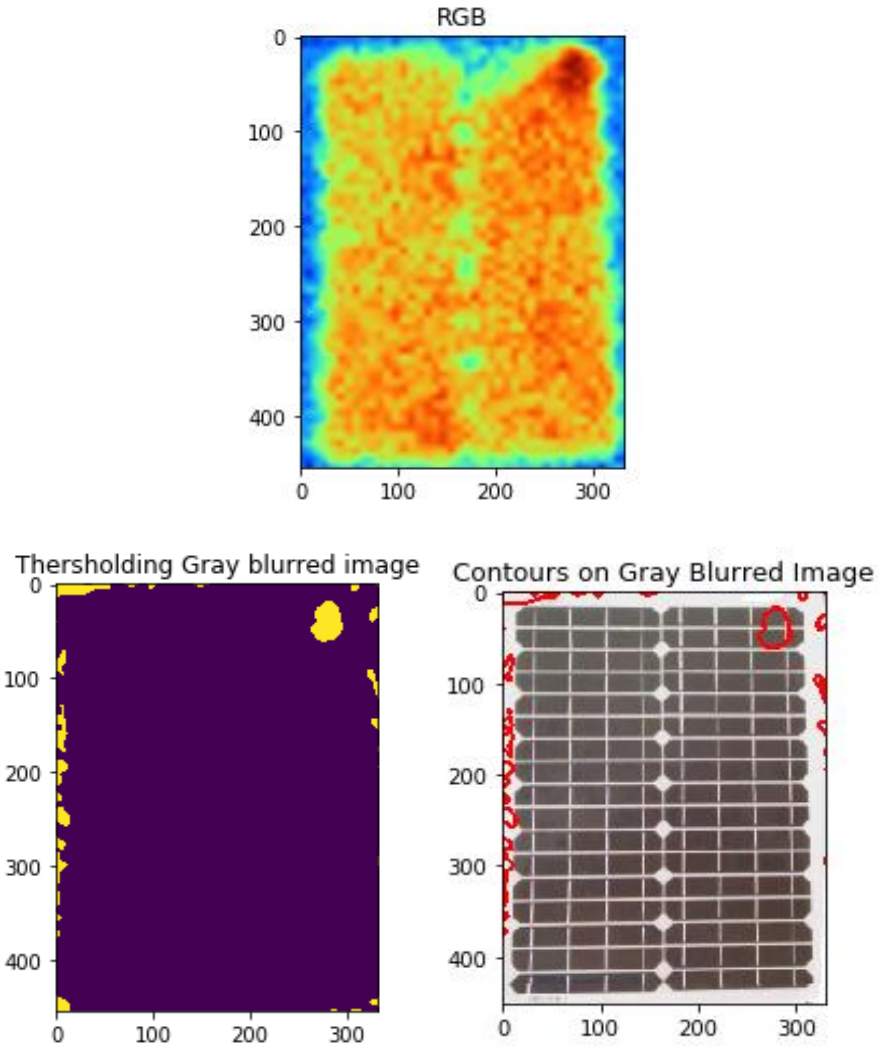

Fig.4.13: RGB, Thresholding Gray Blurred and Contours on Gray blurred images of Mono-Silicon 3 PV module

And the contour shows that the hotspot covers 0.6652527960625038 %. This also is centered on a cell gridline. The hotspots are mostly centered on cell gridlines.

4.7 Summary

The conventional analyzation of performance degradation has matched the faults found in the thermogram analyzation of the PV modules. The current, voltage profile and I-V characteristic curve remains consistent with the result of visual and IR thermographic analyzation of the PV modules. The soldering joints also contribute to the power loss these PV modules, while it is very prominently visible that the relation between hotspot and performance degradation of PV modules exist and because of higher hotspot amount the PV modules have higher degradation rate. Lastly the area of the detected hotspot was calculated and shown on the respective module surfaces to correlate with the visual inspection.

Chapter 5
Conclusion

The main objective of this thesis was to determine the performances of various PV modules and the detection of possible hotspots and defects using infrared thermography which was done with success and it was taken a further step of making it as a capable standard method to determine the quality of PV system and the total degradation percentage of the PV module. At first, Performance measurement of the PV modules was done using I-V characteristic method for determination of degradation and its effect on PV modules. This method was also used for possible defects detection in the PV modules. Visual inspection was done to determine the defects such as cell cracks, junction box, resistive solder bonds, discolored cell gridlines, absence of bypass diode, damage of front glass etc. that can be seen with eyes easily. After visual inspection, with the help of IR camera, thermal images of the PV modules were taken for further defect detection. In thermal images, it was seen that the defects that were seen on different places of PV modules' surfaces during visual inspection, hot spots occurred on those places radiating excessive heat which is counted as defect. Also, Junction box connections of different PV modules were checked by thermography in dark condition.

As a result, it was seen that junction box soldering caused resistive heat loss which is another defect of PV system. After that, a linear correlation of temperature difference was found between hotspot and the ambient temperature with respect to performance degradation. It was observed that the temperature of the hotspot region increases as the performance of PV module worsens. In terms of performance degradation, temperature difference was also observed and the modules had a higher percentage of degradation, as the temperature difference rose. After that, in order to detect the hotspot from its digital infrared image on the panel, an algorithm was implemented to determine how much defect is found over an area of PV modules with hotspot thermal images. It was also observed that increase in the number of hotspots on PV modules' surfaces doesn't increase degradation. The bigger the area & the higher the temperature difference, performance of PV system degrades with time.

As consumers use PV systems for their household without knowing much details about the quality of the PV modules, this method can help them measuring the quality of PV system. Which is why this method can become a standard measurement for PV systems. As for manufacturers, they can build close to zero-defect or standard quality PV systems preventing shortfalls and fulfilling consumers' demands with saving energy production cost. Also, PV

systems exported from other countries can be examined easily with this method. Sometimes PV systems get damaged in both post manufacturing and during shipping. Hence, in future, this method can be an easy, safe and efficient technique for checking PV system quality in both Bangladesh and other countries.

References

1. John A. Tsanakas, Long Ha, Claudia Buerhop. (2016). Faults and infrared thermographic diagnosis in operating c-Si photovoltaic modules: A review of research and future challenges. Renewable and Sustainable Energy Reviews62 (2016)695–709.
2. Available : http://www.bpdb.gov.bd [Accessed: 14-Nov-18
3. SHAKIR-ul haque Khan, TOWFIQ-ur-Rahman, SHAHADAT Hossain. (2012). A brief study of the prospect of solar energy in generation of electricity in bangladesh. Retrieved from http://www.cyberjournals.com/Papers/Jun2012/02.pdf
4. Chakma,Jagaran.(2018,June 24). Solar power capacity reaches 218MW.The Daily Star. Retrieved from https://www.thedailystar.net/business/solar-power-capacity-reaches-218mw-1594513
5. Phinikarides A, Kindyni N, Makrides G, Georghiou GE. Review of photovoltaic degradation rate methodologies. Renew Sustain Energy Rev2014; 40:143–52.
6. Sharma V, Chandel SS. Performance and degradation analysis for long-term reliability of solar photovoltaic systems: a review. Renew Sustain Energy Rev 2013; 27:753–67.
7. Tsanakas JA,Vannier G, Plissonnier A, Ha L, Barruel F. Fault diagnosis and classification of large-scale photovoltaic plants through aerial orthophoto thermal mapping. In: Proceedings of the 31st European photovoltaic solar energy conference and exhibition (EUPVSEC). Hamburg, Germany; 2015.
8. Tsanakas JA, Chrysostomou D, Botsaris PN, Gasteratos A. Fault diagnosis of photovoltaic modules through image processing and Canny edge detection on field thermographic measurements. Int J Sustain Energy 2015; 34:6.
9. Maldague XPV. Getting started with thermography for nondestructive testing. Theory and practice of infrared technology for nondestructive testing. 1st ed. New York: Wiley-Interscience; 2001 [chapter 1].
10. Sakagami, T., and Kubo, S., 2002, "Applications of Pulse Heating Thermography and Lock-In Thermography to Quantitative Nondestructive Evaluations,"Infrared Phys. Technol., 43_3–5_, pp. 211–218.
11. Djordjevic S, Parlevliet D,Jennings P. Detectable faults on recently installed solar modules in western Australia. Renew Energy 2014; 67:215–21.
12. Köntges M, Siebert M, Hinken D, Eitner U, Bothe K, Potthof T. Quantitative analysis of PV-modules by electroluminescence images for quality control. In: Proceedings of

the 24th European photovoltaic solar energy conference and exhibition (EU PVSEC). Hamburg, Germany; 2009.

13. Kontges M, Kurtz S, Packard C, Jahn U, Berger KA, Kato K, et al. Performance and reliability of photovoltaic systems – subtask 3.2: review of failures of photovoltaic modules. External final report by international energy agency (IEA) for photovoltaic power systems programme (PVPS).2014.

14. C. Schuss et al., "Detecting Defects in Photovoltaic Cells and Panels and Evaluating the Impact on Output Performances," in IEEE Transactions on Instrumentation and Measurement, vol. 65, no. 5, pp. 1108-1119, May 2016.

15. Kasap,Safa & Sinha,Ravindra.(2013).Optoelectronics and Photonics: Principles and Practice (Second Edition).

16. Tucci, Mario & Izzi, Massimo. (2013). High efficiency monocrystalline silicon solar cells: reaching the theoretical limit.

17. Salazar AM, Macabebe EQB, "Hotspots Detection in Photovoltaic Modules Using Infrared Thermography", IEEE International Conference on Management of Innovation and Technology, Bangkok, Thailand, vol. 70, pp. 1–5,2016.

18. Tsanakas JA, Botsaris PN, "Passive and active thermographic assessment as a tool for condition-based performance monitoring of photovoltaic modules," ASME J. Sol. Energy Eng., vol. 133, May 2011.

19. Felipe Freire, Steve Melcher, Clark G. Hochgraf, and Santosh K. Kurinec. Degradation analysis of an operating PV module on a Farm Sanctuary. Journal of Renewable and Sustainable Energy

20. García, Miguel & Marroyo, Luis & Pigueiras, Eduardo & Marcos, Javier & Perez, Miguel. (2013). Observed degradation in photovoltaic plants affected by hot-spots. Progress in Photovoltaics: Research and Applications. 22. 10.1002/pip.2393.

21. C. Buerhop, H. Scheuerpflug, R. Weißmann: The Role of Infrared Emissivity Of Glass on IR-Imaging of PV-Plants, Proc. 26th EUPVSEC (WIP, Hamburg, Germany, 2011), pp. 3413 – 3416

22. Retrieved from: https://datasheets.maximintegrated.com/en/ds/DS18B20.pdf

23. Retrieved from: https://www.fluke.com/en/learn/best-practices/measurement-basics/thermography/how-infrared-cameras-work

Appendix

Contour Detection of Panels

Contour Detection on thermographs of M1

In [56]:
```
import cv2
import numpy as np
import matplotlib.pyplot as plt
%matplotlib inline
# Load a color image
img = cv2.imread("33.jpg")
h,w = img.shape[:2]
whole_area_mask = np.ones((h, w), np.uint8)
ret, thresh = cv2.threshold(whole_area_mask,0,255,cv2.THRESH_BINARY+cv2.THRESH_OTSU)
_, contours, hierarchy = cv2.findContours(thresh,cv2.RETR_TREE,cv2.CHAIN_APPROX_NONE)
cnt = max(contours, key=cv2.contourArea)
whole_area = cv2.contourArea(cnt)
gray = cv2.cvtColor(img, cv2.COLOR_BGR2GRAY)
plt.imshow(cv2.cvtColor(img, cv2.COLOR_BGR2RGB))
plt.title('RGB')
print(1)
plt.figure()
plt.title('Gray')
plt.imshow(gray, cmap='gray')
```

```
1
```

Out[56]: <matplotlib.image.AxesImage at 0x7ff63edfc5c0>

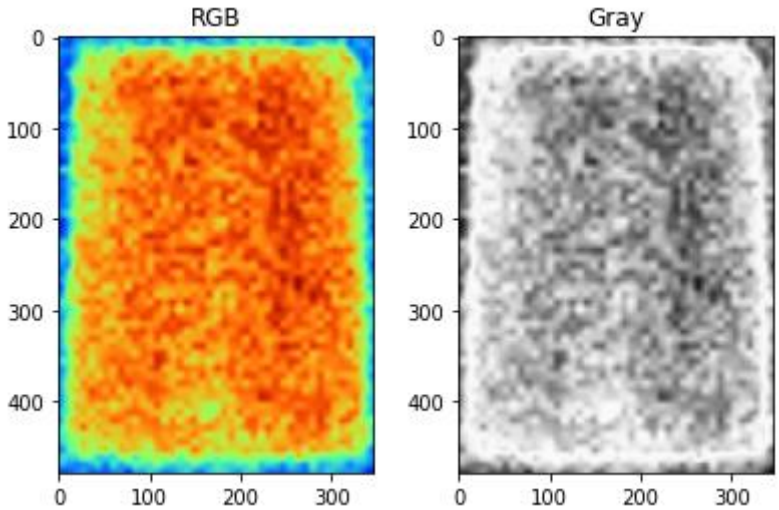

```
In [57]: templateWindowSize = 7
searchWindowSize = 21
blur = cv2.fastNlMeansDenoising(gray, None,10,templateWindowSize,searchWindowSize)
plt.imshow(blur, cmap='gray')
plt.title('Bluring gray image')

Out[57]: Text(0.5,1,'Bluring gray image')
```

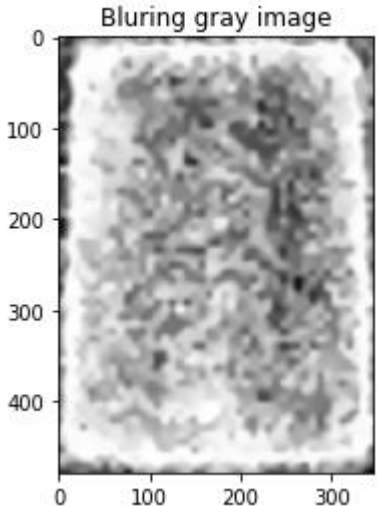


```
In [58]: thresh = cv2.threshold(blur,100,255,cv2.THRESH_BINARY_INV)[1]
plt.imshow(thresh)
plt.title('Thersholding Gray blurred image')
Out[58]: Text(0.5,1,'Thersholding Gray blurred image')
```

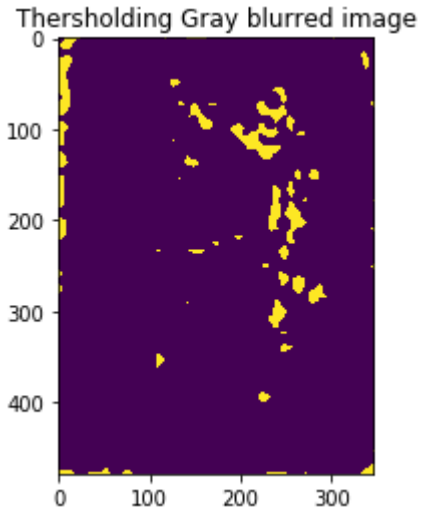

```
In [63]: (cnting, contours, _) = cv2.findContours(thresh.copy(), cv2.RETR_TREE,
cv2.CHAIN_APPROX
contours = sorted(contours, key=cv2.contourArea, reverse=True) #[::2]
img2 = cv2.imread("m2-01.jpg") #IR_02564
out = cv2.drawContours(img2, contours, -1, (255,0,0), 3)
i = 0
area = 0
total_area = 0
for contour in contours:
#area = (cv2.contourArea(contour)/(img.shape[0]*img.shape[1])*100)
#if area>0.01:
cnt = cv2.contourArea(contour)
if cnt>50:
print(str((100*cnt)/whole_area),"% ",i)
i+=1
total_area+= cnt
print('Total defect: ',((100*total_area)/whole_area),'%')
#plt.imshow(cv2.cvtColor(out, cv2.COLOR_BGR2RGB))
plt.imshow(out)
plt.title('Contours on Gray Blurred Image')
0.5221029652537748 % 0
0.39294160451155175 % 1
0.2768176581165484 % 2
0.21860408707780002 % 3
0.18403977927354315 % 4
0.17373112606876479 % 5
0.16251288581650597 % 6
0.15796495057910376 % 7
0.1264325995997817 % 8
0.1118792068400946 % 9
0.10975683706264022 % 10
0.10035777090534231 % 11
0.09641622703292706 % 12
0.0873203565581226 % 13
0.06276150627615062 % 14
0.06033594081620278 % 15
0.05912315808622885 % 16
```

0.05851676672124189 % 17

0.057607179673761444 % 18

0.057607179673761444 % 19

0.05487841853132011 % 20

0.05396883148383967 % 21

0.05033048329391789 % 22

0.045479352374022196 % 23

0.0421441998665939 % 24

0.034564307804256865 % 25

Total defect: 3.5992359468801163 %

Out[63]: Text(0.5,1,'Contours on Gray Blurred Image')

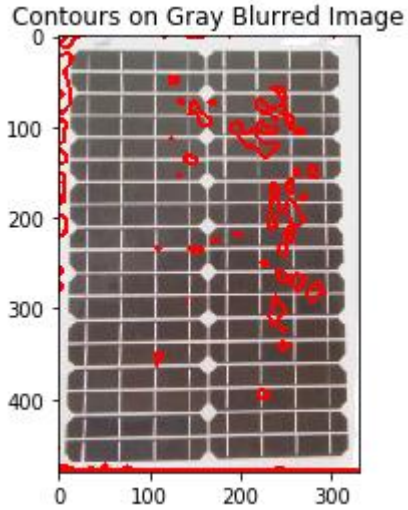

Contour Detection on thermographs of M2

In [1]:
```
import cv2
import numpy as np
import matplotlib.pyplot as plt
%matplotlib inline
# Load a color image
img = cv2.imread("32.jpg")
h,w = img.shape[:2]
whole_area_mask = np.ones((h, w), np.uint8)
ret, thresh = cv2.threshold(whole_area_mask,0,255,cv2.THRESH_BINARY+cv2.THRESH_OTSU)
_, contours, hierarchy = cv2.findContours(thresh,cv2.RETR_TREE,cv2.CHAIN_APPROX_NONE)
cnt = max(contours, key=cv2.contourArea)
whole_area = cv2.contourArea(cnt)
gray = cv2.cvtColor(img, cv2.COLOR_BGR2GRAY)
plt.imshow(cv2.cvtColor(img, cv2.COLOR_BGR2RGB))
plt.title('RGB')
print(1)
plt.figure()
plt.title('Gray')
plt.imshow(gray, cmap='gray')
```

Out[1]: <matplotlib.image.AxesImage at 0x7fd3335bda58>

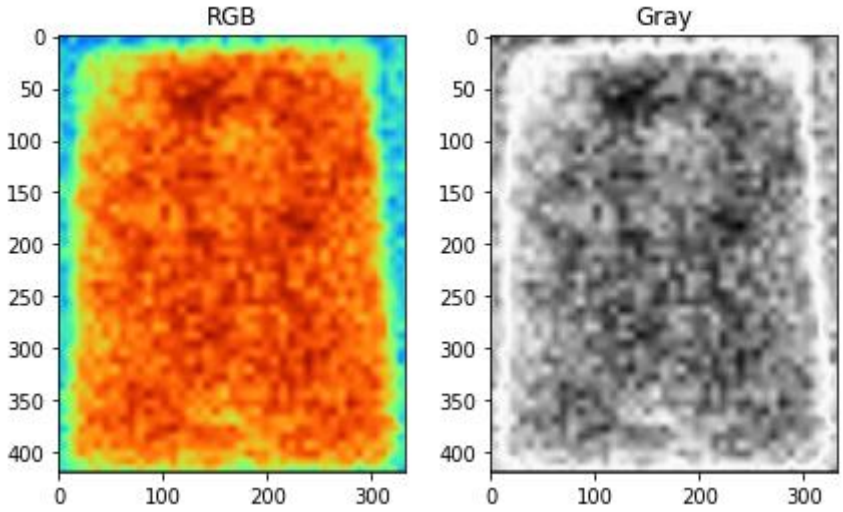

In [2]: templateWindowSize = 7
searchWindowSize = 21

```
blur = cv2.fastNlMeansDenoising(gray, None,10,templateWindowSize,searchWindowSize)
plt.imshow(blur, cmap='gray')
plt.title('Bluring gray image')
```

Out[2]: Text(0.5,1,'Bluring gray image')

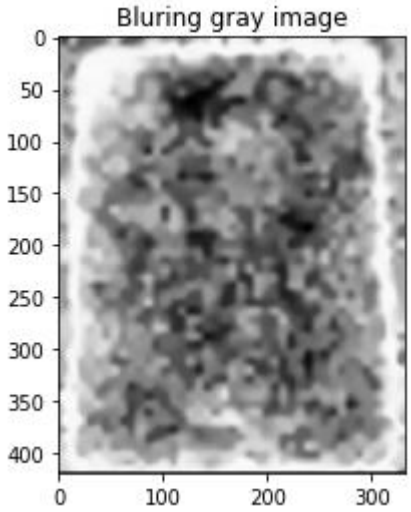

In [3]: thresh = cv2.threshold(blur,100,255,cv2.THRESH_BINARY_INV)[1]
plt.imshow(thresh)
plt.title('Thersholding Gray blurred image')
Out[3]: Text(0.5,1,'Thersholding Gray blurred image')

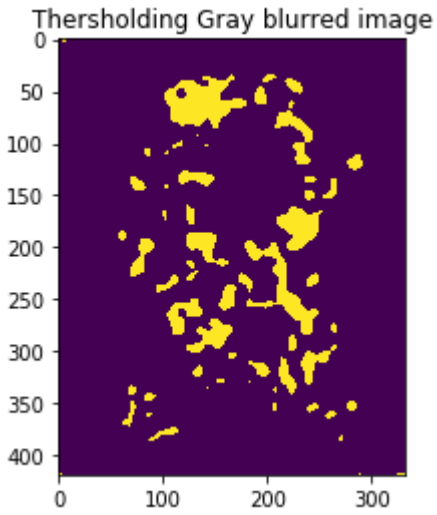

```
In [4]: (cnting, contours, _) = cv2.findContours(thresh.copy(), cv2.RETR_TREE,
cv2.CHAIN_APPROX_
contours = sorted(contours, key=cv2.contourArea, reverse=True) #[::2]
img2 = cv2.imread("m2-01.jpg") #IR_02564
out = cv2.drawContours(img2, contours, -1, (255,0,0), 3)
i = 0
area = 0
total_area = 0
for contour in contours:
#area = (cv2.contourArea(contour)/(img.shape[0]*img.shape[1])*100)
#if area>0.01:
cnt = cv2.contourArea(contour)
if cnt>50:
print(str((100*cnt)/whole_area),"% ",i)
i+=1
total_area+= cnt
print('Total defect: ',((100*total_area)/whole_area),'%')
#plt.imshow(cv2.cvtColor(out, cv2.COLOR_BGR2RGB))
plt.imshow(out)
plt.title('Contours on Gray Blurred Image')
1.6018619934282585 % 0
1.0437683749351472 % 1
0.7501297054245691 % 2
0.45541015737591517 % 3
0.41181472300685995 % 4
0.3847927595549663 % 5
0.30192540496915893 % 6
0.2900357410503257 % 7
0.23383005707038682 % 8
0.22518302876578083 % 9
0.20644780077246785 % 10
0.19527872254568512 % 11
0.13907303856574624 % 12
0.10196287542514555 % 13
0.09872023981091832 % 14
0.09835994696489307 % 15
0.09547760419669107 % 16
```

0.08791145443016084 % 17

0.08610999020003458 % 18

0.08466881881593359 % 19

0.0832276474318326 % 20

0.07998501181760535 % 21

0.07386003343517611 % 22

0.07241886205107512 % 23

0.06917622643684787 % 24

0.06305124805441863 % 25

0.05620568397993889 % 26

0.04791894852135816 % 27

0.04539689859918142 % 28

0.04107338444687842 % 29

0.03999250590880268 % 30

0.03783074883265118 % 31

0.03674987029457543 % 32

0.03674987029457543 % 33

0.03638957744855018 % 34

Total defect: 8.03380988067101 %

Out[4]: Text(0.5,1,'Contours on Gray Blurred Image')

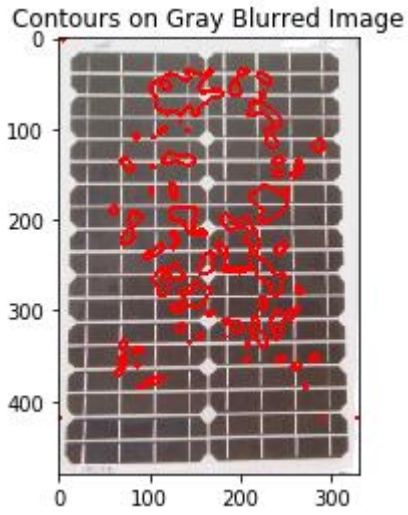

Contour Detection on thermographs M3

In [5]:
```
import cv2
import numpy as np
import matplotlib.pyplot as plt
%matplotlib inline
# Load a color image
img = cv2.imread("41.jpg")
h,w = img.shape[:2]
whole_area_mask = np.ones((h, w), np.uint8)
ret, thresh = cv2.threshold(whole_area_mask,0,255,cv2.THRESH_BINARY+cv2.THRESH_OTSU)
_, contours, hierarchy = cv2.findContours(thresh,cv2.RETR_TREE,cv2.CHAIN_APPROX_NONE)
cnt = max(contours, key=cv2.contourArea)
whole_area = cv2.contourArea(cnt)
gray = cv2.cvtColor(img, cv2.COLOR_BGR2GRAY)
plt.imshow(cv2.cvtColor(img, cv2.COLOR_BGR2RGB))
plt.title('RGB')
print(1)
plt.figure()
plt.title('Gray')
plt.imshow(gray, cmap='gray')
```

Out[5]: <matplotlib.image.AxesImage at 0x7fd332ff59e8>

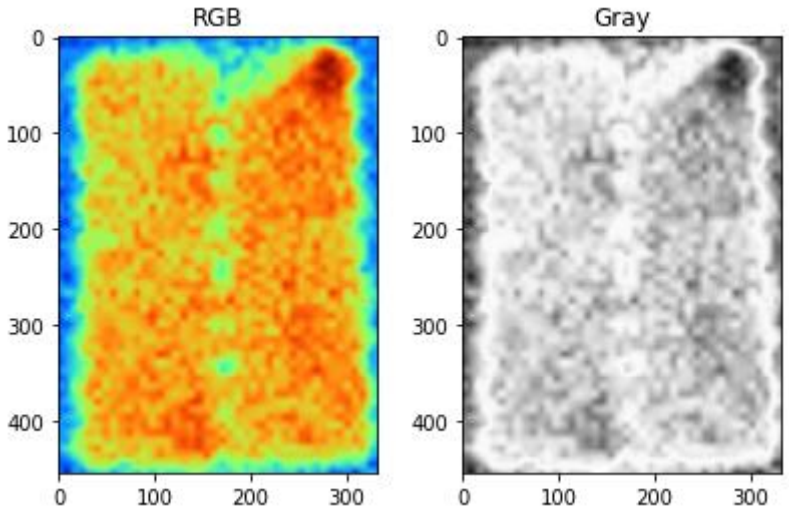

In [6]:
```
templateWindowSize = 7
searchWindowSize = 21
```

```
blur = cv2.fastNlMeansDenoising(gray, None,10,templateWindowSize,searchWindowSize)
plt.imshow(blur, cmap='gray')
plt.title('Bluring gray image')
```

Out[6]: Text(0.5,1,'Bluring gray image')

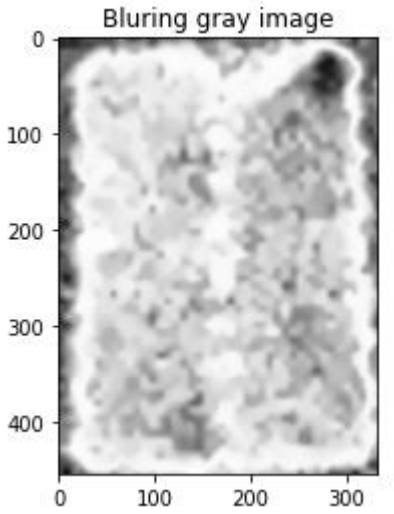

In [7]:
```
thresh = cv2.threshold(blur,100,255,cv2.THRESH_BINARY_INV)[1]
plt.imshow(thresh)
plt.title('Thersholding Gray blurred image')
```

Out[7]: Text(0.5,1,'Thersholding Gray blurred image')

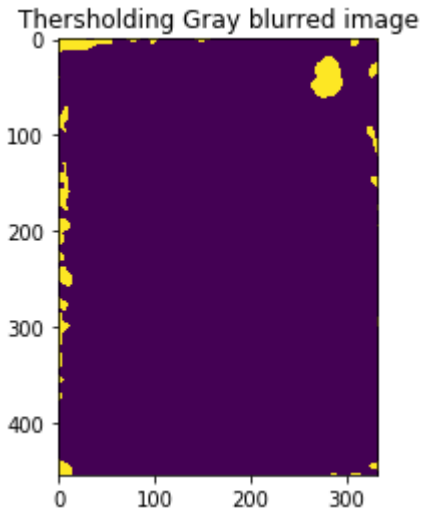

In [8]:
```
(cnting, contours, _) = cv2.findContours(thresh.copy(), cv2.RETR_TREE,
cv2.CHAIN_APPROX_
contours = sorted(contours, key=cv2.contourArea, reverse=True) #[::2]
```

```
img2 = cv2.imread("m2-01.jpg") #IR_02564
out = cv2.drawContours(img2, contours, -1, (255,0,0), 3)
i = 0
area = 0
total_area = 0
for contour in contours:
#area = (cv2.contourArea(contour)/(img.shape[0]*img.shape[1])*100)
#if area>0.01:
cnt = cv2.contourArea(contour)
if cnt>50:
print(str((100*cnt)/whole_area),"% ",i)
i+=1
total_area+= cnt
print('Total defect: ',((100*total_area)/whole_area),'%')
#plt.imshow(cv2.cvtColor(out, cv2.COLOR_BGR2RGB))
plt.imshow(out)
plt.title('Contours on Gray Blurred Image')
```

```
0.6652527960625038 % 0
0.33579426848869237 % 1
0.17506652527960626 % 2
0.16006082311278286 % 3
0.13338401926065238 % 4
0.12404713791240672 % 5
0.1067072154085219 % 6
0.09903763430103439 % 7
0.08669961251942405 % 8
0.06669200963032619 % 9
0.05935588857099031 % 10
0.046350946693076704 % 11
0.03601368520037614 % 12
Total defect: 2.295872431523979 %
```

Out[8]: Text(0.5,1,'Contours on Gray Blurred Image')

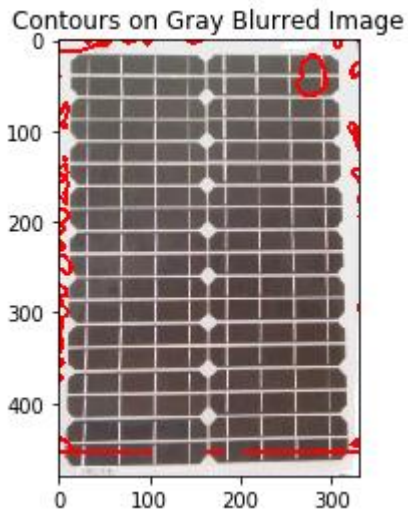

Contour Detection on thermograph P3

In [50]:
```
import cv2
import numpy as np
import matplotlib.pyplot as plt
%matplotlib inline
# Load a color image
img = cv2.imread("28.jpg")
h,w = img.shape[:2]
whole_area_mask = np.ones((h, w), np.uint8)
ret, thresh = cv2.threshold(whole_area_mask,0,255,cv2.THRESH_BINARY+cv2.THRESH_OTSU)
_, contours, hierarchy = cv2.findContours(thresh,cv2.RETR_TREE,cv2.CHAIN_APPROX_NONE)
cnt = max(contours, key=cv2.contourArea)
whole_area = cv2.contourArea(cnt)
gray = cv2.cvtColor(img, cv2.COLOR_BGR2GRAY)
plt.imshow(cv2.cvtColor(img, cv2.COLOR_BGR2RGB))
plt.title('RGB')
print(1)
plt.figure()
plt.title('Gray')
plt.imshow(gray, cmap='gray')
```

Out[50]: <matplotlib.image.AxesImage at 0x7ff63f172e48>

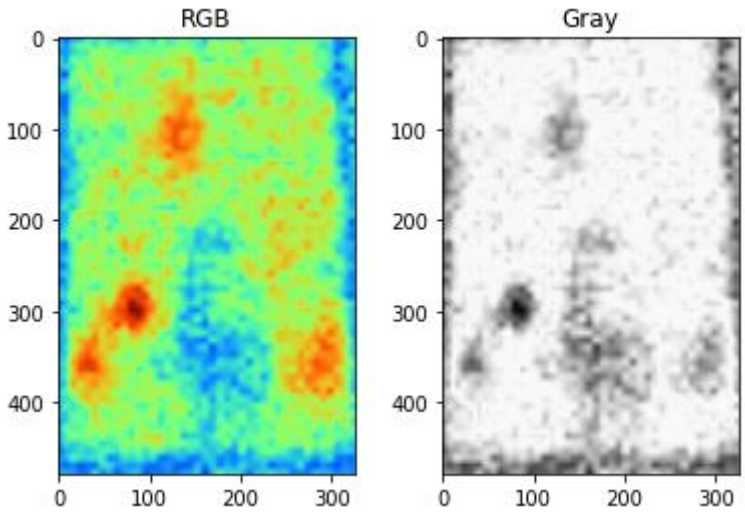

In [51]: templateWindowSize = 7

searchWindowSize = 21

blur = cv2.fastNlMeansDenoising(gray, None,10,templateWindowSize,searchWindowSize)

plt.imshow(blur, cmap='gray')

plt.title('Bluring gray image')

Out[51]: Text(0.5,1,'Bluring gray image')

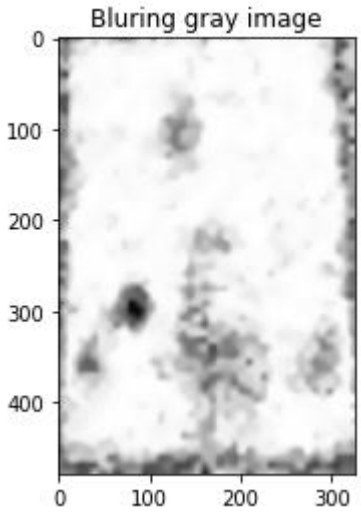

In [52]: thresh = cv2.threshold(blur,100,255,cv2.THRESH_BINARY_INV)[1]

plt.imshow(thresh)

plt.title('Thersholding Gray blurred image')

Out[52]: Text(0.5,1,'Thersholding Gray blurred image')

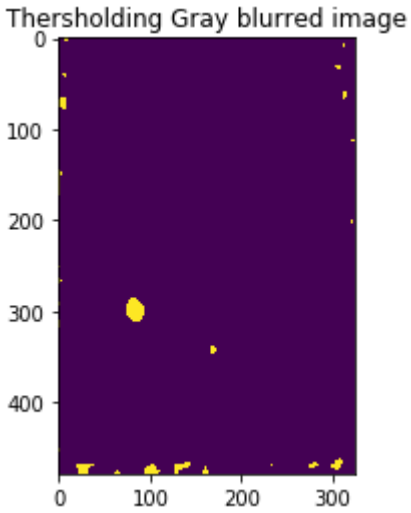

In [55]:
```
(cnting, contours, _) = cv2.findContours(thresh.copy(), cv2.RETR_TREE,
cv2.CHAIN_APPROX
contours = sorted(contours, key=cv2.contourArea, reverse=True)[1:]
img2 = cv2.imread("IR_02564.jpg") #m2-01
out = cv2.drawContours(img2, contours, -1, (255,0,0), 3)
i = 0
area = 0
total_area = 0
for contour in contours:
#area = (cv2.contourArea(contour)/(img.shape[0]*img.shape[1])*100)
#if area>0.01:
cnt = cv2.contourArea(contour)
if cnt>50:
print(str((100*cnt)/whole_area),"% ",i)
i+=1
total_area+= cnt
print('Total defect: ',((100*total_area)/whole_area),'%')
#plt.imshow(cv2.cvtColor(out, cv2.COLOR_BGR2RGB))
plt.imshow(out)
plt.title('Contours on Gray Blurred Image')
```

0.24750563244287094 % 0

0.05407145156099131 % 1

0.04602510460251046 % 2

0.03379465722561957 % 3

Total defect: 0.4905053105889926 %

Out[55]: Text(0.5,1,'Contours on Gray Blurred Image')